Journal of Aeronautics, Astronautics and Aviation, Vol. 55, No. 3, pp. 385 – 414 (2023)
DOI: https://doi.org/10.6125/JoAAA.202309_55(3).09

Review of Hollow Cathode Discharge: Exploring Advanced Design and Optimization

Jordan H. Hsieh [1] and Yueh-Heng Li [1, 2 *]

[1] *Department of Aeronautics and Astronautics, National Cheng Kung University, Tainan, 70101, Taiwan.*
[2] *International Doctoral Degree Program on Energy Engineering, National Cheng Kung University, Tainan, 70101, Taiwan*

ABSTRACT

Electric propulsion has seen significant development over the years, resulting in its popularity due to its expanded capabilities in satellite constellation management and orbital transfer vehicles. Hollow cathodes have become an extensively utilized source of electrons for propellant ionization and ion beam neutralization in electric propulsion systems. This paper reviews the hollow cathode discharge and the recent advancements and progress in hollow cathode technology to highlight the key areas that require further research. The classic hollow cathode design, which features an external heater and has been widely used in flight programs, is discussed, followed by a focus on heaterless hollow cathodes, which have recently gained publicity. The critical aspects of low-current and high-current hollow cathode operation, including the emitter material and self-heating mechanisms, are highlighted in this review, each facing unique challenges. Future challenges for hollow cathodes involve creating chemically stable, long-lasting materials with low work function, optimizing the design to reduce ion yield and erosion, and ongoing modeling of cathode operation and plasma instabilities.

Keywords: Electric Propulsion, Hollow cathode, Mode transition, Instabilities, Emitter

NOMENCLATURE

A	theoretical value
A_c	cross-sectional area
D	material-specific modification
E	electric field
EP	electric propulsion
e	charge
$H(T)$	total heat lost by the insert
HC	hollow cathode
HHC	heaterless hollow cathode
I_e	discharge current
I_i	Bohm current
I_r	random electron flux
IAT	ion-acoustic turbulence
J	thermionic emission current density
k	Boltzmann constant
L	average conduction length
P_i	ion heating to the insert surface
P_e	electron heating to the insert surface
PPU	power processing unit
R	resistance of the plasma
SCCM	standard cubic centimeter per minute
T	temperature
T_{eV}	electron temperature
U	ionization potential
α	measured constant
ε_0	vacuum permittivity
η	resistivity of the plasma
$\emptyset_r$	reported work function

Manuscript received, August 4, 2023, final revision, August 18, 2023
* To whom correspondence should be addressed, E-mail: yueheng@mail.ncku.edu.tw

$\emptyset_s$ sheath potential
$\emptyset_{wf}$ work function

I. INTRODUCTION

Electric propulsion (EP) has a rich history dating back to the early 1900s when Russian scientist Konstantin Tsiolkovsky first introduced the concept of using electrically charged particles to propel spacecraft [1]. However, it was not until the 1960s that the first satellite with EP, the SERT-1, was sent to space [2]. Since then, EP has developed significantly, branching into various categories and being widely used in the satellite field [3-8]. Compared to traditional chemical propulsion systems [9], EP systems offer several advantages, such as higher specific impulse, efficiency, and longer operating lifetimes. From the plasma discharge perspective, EP can be classified into steady and unsteady categories. Steady EP involves continuous firing for a specific duration and includes systems such as the arc jet [10], ion thruster [11-13], magneto plasma dynamic thruster (MPDT) [14, 15], Hall thruster [16-19], helicon plasma thruster [20], and field-emission electric propulsion (FEEP) [21, 22]. Unsteady EP, on the other hand, involves pulsed firings that accumulate to achieve a desired impulse and includes systems such as vacuum arc thruster (VAT) [23] and pulsed plasma thruster (PPT) [24, 25].

EP has gained popularity in satellite constellations due to its expanded capabilities, including orbital maneuvering, station keeping, collision avoidance, and de-orbiting [26-37]. These systems are being used for a range of services provided by small satellites, such as internet connectivity and remote sensing. A prominent example is SpaceX's Starlink constellation, which employs Hall thrusters for orbital maneuvering and has recently switched its propellant to argon. EP has also been recently utilized in an asteroid deflection mission. NASA's Double Asteroid Redirection Test (DART) mission [38], which aimed to demonstrate asteroid deflection by a kinetic impactor, utilized an ion thruster (NEXT–C) with xenon as the propellant. The impactor satellite collided with Dimorphos, the target asteroid, in 2022 at a speed of approximately 6.1 kilometers per second.

Hollow cathodes (HC) have been a fundamental component of EP systems since the 1960s [39]. These gas discharge devices are commonly utilized in steady EP systems as an electron source for propellant ionization and ion beam neutralization via thermionic emission. The cylindrical-shaped devices consist of a hollow cylinder with a cathode electrode at its center. In order to reach the necessary temperature for thermionic emission, the cathode is heated using either an external heater (known as Ohmic heating) or plasma discharge through ion and electron heating. Following heating, the electrons in the HC are subsequently extracted from the cathode via the plasma potential.

The unique characteristics of the HC make it an ideal choice for EP. It is known for its low power consumption rate, high ionization efficiency, and ability to operate for long periods without maintenance [40]. Depending on the emitter material, HCs can also operate on various propellants, such as xenon, krypton, argon, nitrogen, or iodine [41]. Recently, researchers have focused on enhancing the performance of the HC by developing new materials and designs [42], which include the use of advanced low work function ceramics [43] and heating methodologies [44, 45] to improve durability and reliability.

The rapidly growing field of HC technology has become increasingly important in space applications. However, despite the active advancements, areas in HC technology still require a more profound understanding of plasma behavior and optimal cathode design. Moreover, as HC technology is applied more widely in real-world contexts, it is crucial to assess this area's progress and persisting challenges comprehensively. This paper seeks to address this need by reviewing the state-of-the-art HC technology and identifying the areas where future research efforts should be directed. Building upon the review conducted by Lev et al. in 2019 [46], this paper aims to present the advancements and challenges in the field of HC technology, emphasizing the unique challenges faced by both low-current and high-current HC operations. In addition, the paper will discuss the classic HC design with an external heater, as well as the increasingly popular heaterless hollow cathodes (HHC), which have gained attention for their potential in space applications. Ultimately, this review aims to provide an overview of the current state of HC technology, highlight the key areas that require further research, and serve as a guide for future studies and developments in the field.

II. HOLLOW CATHODE

HCs provide electrons for propellant ionizing and ion bean neutralizing in the ion and Hall thruster. The core concept of the HC is to emit electrons through a low work function material, often called an insert or emitter, through thermionic emission. The thermionic electrons then ionize a portion of propellant feeds through the insert region, usually noble gas or iodine, and are extracted to the plume region by the plasma potential formulated by the keeper or anode.

Figure 1 presents the configuration of a classical HC with an external heater. The HC configuration typically consists of a cylindrical cathode tube made of refractory metals or graphite with a hollow center. Low work function insert within the cathode tube is heated by either an external heater or plasma to reach the thermionic emission temperature. The cathode tube is surrounded by a keeper, which encloses the cathode tube and forms a narrow annular gap between it.

The keeper is an essential component of the HC that serves several vital functions [48]. First, it facilitates the cathode discharge initiation and ensures its stable operation. Second, it helps maintain the cathode temperature and operation during temporary interruptions in the discharge. Last, it protects the cathode orifice plate and external heater from damage caused by high-energy ion bombardment, which could otherwise limit the lifespan of the cathode. The keeper electrode is normally

biased positively relative to the cathode. This positive bias helps initiate the discharge during start-up and reduces the ion bombardment energy during regular operation. The life of the keeper electrode is crucial for the overall lifespan of the cathode and EP system.

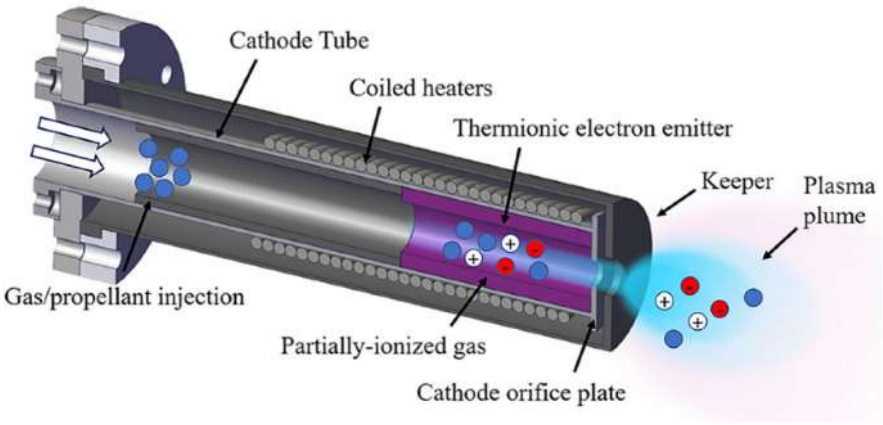

Figure 1 The configuration of hollow cathode [47].

The injecting propellant through the cathode generates a high-density, cold plasma inside the high neutral pressure region. The electron temperature is low, while the plasma and neutral densities are high; this leads to a low plasma potential in the insert region and a reduction in ion bombardment energy, increasing the cathode's life. Additionally, the high-density plasma eliminates space charge effects, which can limit the electron emission current density. The cathode insert can also be heat shielded by the cylindrical geometry, reducing radiation losses and decreasing the power needed to maintain the required temperature for electron emission.

THERMIONIC EMISSION

In the HC, electrons are introduced through thermionic emission from the insert surface. The process of thermionic emission by cathodes can be roughly described by the Richardson–Dushman equation, which describes the relationship between temperature, work function, and the rate of electron emission from a heated surface [49, 50]:

$$J = AT^2 e^{-e\emptyset_{wf}/kT} \quad (1)$$

where J is the thermionic emission current density, T is the temperature in kelvins, e is the charge, $\emptyset_{wf}$ is the work function, k is the Boltzmann constant, and A is a theoretical value of $120\,A/cm^2K^2$. The theoretical value of A may be verified due to several factors, such as the crustal structure of the emitter surface [48]. A temperature correction has been introduced for the work function of thermionic electron emitters used in HCs. This correction was addressed in reference [51]:

$$\emptyset_{wf} = \emptyset_r + \alpha T \quad (2)$$

where $\emptyset_r$ is the classically reported work function of the emitter, and α is the measured constant in the experiment. Inserting this temperature correction in Eq. (1) can give [48]:

$$J = DT^2 e^{-e\emptyset_r/kT} \quad (3)$$

where $D = Ae^{-e\alpha/k}$ is a material-specific modification to the Richardson-Dushman equation.

The Richardson-Dushman equation accounts for the correlation between the temperature of a heated surface, the work function of the surface material, and the thermionic emission current. However, in HC, especially for the open-ended HC, a strong electric field, i.e., plasma sheath, will formulate in the insert region. As a result, the presence of the electric field will extract more electron current from the inset surface, known as the Schottky effect [52]. The Schottky effect is a phenomenon in which the presence of strong electric fields at the surface reduces the potential barrier that electrons in the conduction band of the material must overcome, effectively resulting in a reduced work function and described as [48, 53]:

$$J = DT^2 \exp\left(\frac{-e\emptyset_r}{kT}\right) exp\left[\left(\frac{e}{kT}\right)\sqrt{\frac{eE}{4\pi\varepsilon_0}}\right] \quad (4)$$

where E is the electric field and ε_0 is the vacuum permittivity. The operating temperature of a HC for a given emission current depends on the emitter material's properties and the surface area for thermionic emission. Different value of $\emptyset_{wf}$ and D for several commonly-utilized emitter materials, such as refractory metal [51, 54-56], barium oxide (BaO) [53, 57, 58], lanthanum hexaboride (LaB_6) [59-61], and calcium aluminate eletride (C12A7) [62-65] can be found in other research.

EMITTER MATERIALS

The exploration and development of the emitter material used for HC can date back to the early 20th century when the first cathode was developed [49]. Early

HCs used oxide-coated cathodes as the emitter material. Oxide layers were deposited on metal filaments like tungsten and nickel [46]. However, it was discovered that these oxide surface layers could be easily sputtered by ion bombardment and evaporate, leading to limited lifetimes in vacuum applications and plasma discharges [46]. Therefore, dispenser cathodes are made to assuage this problem, which continuously re-supplies the low work function surface layer to offer higher emission current densities and longer lifetimes than oxide-coated cathodes [66]. Figure 2 depicts the configuration of a classical flat dispenser cathode, a self-regulating thermionic cathode that uses a porous tungsten reservoir containing a low work function material, such as barium or thorium, to emit electrons when heated. It should be noted that the emitter can also be made in a cylindrical geometry, which is the same as the HC [67]. The unique features of the dispenser cathode make it a valuable tool in research areas such as spacecraft propulsion, plasma physics, and surface science [68-71].

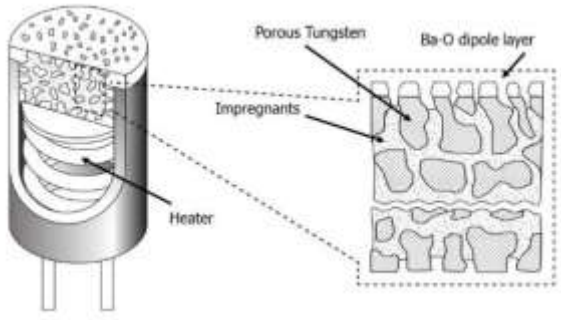

Figure 2 Typical dispenser cathode design with tungsten matrix and impregnants [66].

However, dispenser cathodes are subject to poisoning due to chemistry's involvement in forming the low work function surface [72], which can significantly increase the work function, thereby decreasing the cathode performance. These contaminants can react with the emitter material and form compounds that reduce the emission properties of the cathode [48]. In addition, the emitted current density can decrease over time due to a change in the surface morphology caused by the sputtering of the cathode material [48]. Furthermore, the manufacturing process of dispenser cathodes can be complicated and requires precision to achieve the desired performance. Finally, dispenser cathode can be susceptible to overheating and can degrade when exposed to high temperatures, which possess a maximum continuous current density of about 20 A/cm^2 corresponding to a temperature of about 1200 °C [46]. The relationship between thermionic emission current density and insert temperature for various materials is illustrated in Figure 3. It was observed that when the insert temperature exceeded 1200 °C, the surface evaporation of barium surpassed the supply rate from the tungsten pores, leading to a decrease in surface coverage and an increase in the work function [73, 74].

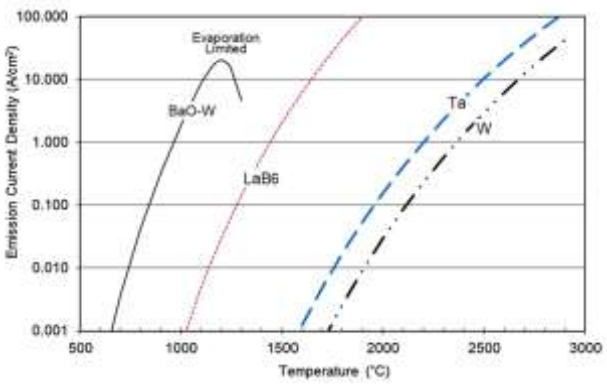

Figure 3 Thermionic electron emission current density versus surface temperature of different materials [46].

Another common thermionic emitter material is lanthanum hexaboride, hereafter simply LaB_6. It is a refractory compound with a low work function, high melting point, and high chemical stability, making it an attractive candidate for cathode applications. First developed as an electron emitter by Lafferty [59] in the 1950s, the use of LaB_6 in HC was subsequently investigated by several researchers [60, 61, 75, 76]. They found that LaB_6-impregnated cathodes performed better than conventional tungsten-impregnated cathodes. To the author's knowledge, the first use case of LaB_6 HCs in space was the Russian SPT Hall thrusters in 1971 [77]. The first reported use case of LaB_6 HC in the United States was by Goebel et al. in 1978 [78].

Several points need to be noticed while utilizing LaB_6 as an emitter. First, although LaB_6 has more chemical stability than BaO-W, it is still quite sensitive to oxygen and water vapor lead by propellent impurity, which can cause poisoning to form lanthanum oxide and boron trioxide, increasing the work function of the emitter [48]. Second, LaB_6 is susceptible to thermal stress, which can cause cracking and failure of the cathode; this is especially problematic in high-power applications where the cathode experiences significant heating and cooling cycles [45, 79]. Finally, using LaB can also lead to boron diffusion into the supporting refractory metal components, such as the cathode tube [80, 81]. Boron diffusion can cause a reduction in the mechanical properties of these materials, leading to premature failure of the HC. Selecting materials that can mitigate boron diffusion from LaB_6, such as graphite, is critical when utilizing LaB_6 as an emitter [59, 82].

One attractive candidate for future electric propulsion applications in space is calcium aluminate electrode (C12A7), first reported by Matsuishi et al. in 2003 [83]. Hosono subsequently researched C12A7, significantly emphasizing developing materials for organic light-emitting diode (OLED) applications [84-86].

The work function of C12A7 has been a subject of debate. However, the intrinsic value of C12A7 is considered 2.4 eV [65]. Molecular dynamics calculations

by Sushko et al. [87] predicted a remarkably low work function of 0.6 eV. However, ultraviolet photoelectron spectroscopy measurements by Toda et al. suggested a much higher work function of 3.7 eV [88]. Field emission studies using single-crystal by Toda et al. in the same study [88] and polycrystalline C12A7 by Kim et al. [89] showed a work function of 0.6 eV in a vacuum diode configuration. At about 900 °C, this thermal field emission showed a higher work function of 2.1 eV [90]. Complicating surface layer effects have led to significant variations in reported work functions, with the initial reports from Hosono et al. and actual HC results varying widely. Figure 4 shows the span of the different work functions of C12A7 in open literature regardless of the melting point or material degradation in high temperatures.

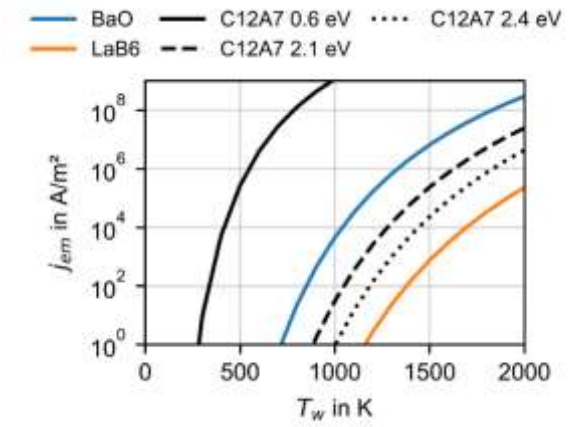

Figure 4 The thermionic emission current densities of C12A7, BaO, and LaB_6 versus surface temperature [91].

Rand et al. introduced C12A7 as a HC emitter in 2010 and demonstrated its operation at currents up to 3.6 A [92, 93]. Later, Rand and Williams developed a more stable version by inserting slivers of electrode into a graphite liner in a tantalum tube, which extended stable operation to several hours at a time [94]. Rand and Williams also show that the C12A7 electrode seems to be compatible with iodine-based on brief tests with no reported signs of insert degradation [62]. A similar study has been conducted by Hua et al. [41]. Drobny et al. made the first tests with tubular C12A7 inserts but encountered instability and insert overheating [95-97] and subsequently reported on the stable operation using a disk-like emitter [43]. McDonald et al. demonstrated the stable operation of a tubular insert C12A7 cathode using a heat sink configuration at low currents of 30-100 mA to prevent insert overheating [98]. Hua et al. presented a stable self-sustained discharge of the C12A7 cathode in a joint operation with a classic SPT-type Hall thruster and reached more than 10 hours without any noticeable degradation [99].

To date, direct comparison between C12A7 and conventional LaB_6 and BaO is still challenging [46]. Although the low operating temperatures of C12A7 provide more freedom in cathode design and material selection, the material faces overheating and discharge voltage instability issues that limit its ability to support lifetime or poisoning testing. Therefore, there is a need for the further advancement of C12A7 HCs to enhance temperature regulation and voltage stability, prolong the operational lifespan, and exhibit material endurance and resistance against plasma contamination for extended mission durations.

SELF-HEATING MECHANISMS

Researchers have studied the phenomenon of self-heating in HCs due to its unique characteristics. When the discharge current exceeds a specific critical value, the cathode can operate without any external heating source, and the emission current and cathode temperature become self-sustained. This paper will review the self-heating operation of the HC, including the physical mechanisms that drive the self-heating process and the various operating parameters that can affect self-heating in HCs.

When operating in a self-heating mode, HC is primarily heated by plasma bombardments in the insert and orifice regions. Three primary heating mechanisms lead to self-heating in HC: electron bombardment, ion bombardment, orifice heating. The heating mechanisms in HCs largely depend on the cathode geometry, discharge current, propellant flow rates, and internal gas pressure. Following the definition made by Goebel et al. [48], in summary, there are two types of HC: open-ended HC and orifice HC, as shown in Figure 5.

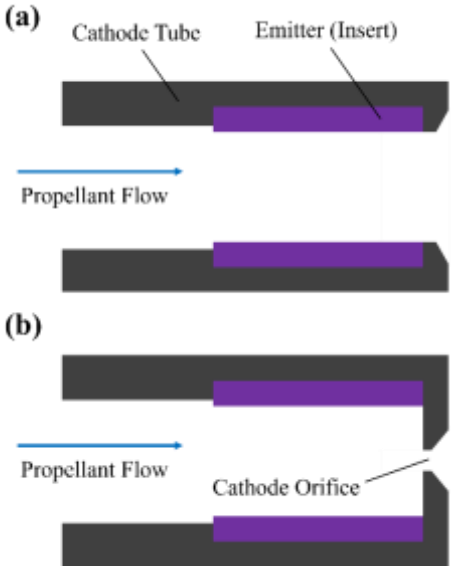

Figure 5 Hollow cathode schematics: (a) open-ended hollow cathode and (b) orifice hollow cathode.

In open-ended HC, i.e., the cathode without orifice, the heating mechanism is dominated by ion bombardment heating, where ions in the cathode insert region fall through the sheath potential at the insert surface, resulting in surface heating by ion bombardment. Estimated by a simple 0-D model, which assumes a reasonably

homogeneous plasma in the insert region, the sheath potential $\emptyset_s$ in the insert region can be described as [48]:

$$\emptyset_s = \frac{H(T)}{I_e} + \frac{5}{2}T_{eV} + \emptyset_{wf} - I_e R \quad (5)$$

where $H(T)$ is the total heat lost by the insert through radiation and conduction, I_e is the HC discharge current, T_{eV} is the electron temperature in volts, and R is the resistance of the plasma, given by $\eta L/A_c$, where η is the resistivity of the plasma, L is the average conduction length, and A_c is the cross-sectional area of the plasma. Eq. (5) is derived by considering the condition $(U + \phi_s) \gg T_{eV}/2$, which is valid in most cases, U denotes ionization potential.

Eq. (5) also shows that the sheath potential is proportional to the electron temperature in the insert region. In an open-ended cathode, the temperature of the electron is usually higher than those of the orifice cathode because of the lower value of neutral gas pressure. The gas pressure within a HC influences the plasma density and profile through collisional effects [100]. As a result, the strong plasma sheath in an open-ended cathode increases the bombarding ion's kinetic energy and limits the electron's total energy deposit to the insert surface. The ion heating P_i and electron heating P_e to the insert surface by bombardment can be described through the 0-D model [48]:

$$P_i = I_i\left(U + \emptyset_s + \frac{T_{eV}}{2} - \emptyset_{wf}\right) \quad (6)$$

$$P_e = \left(2T_{eV} + \emptyset_{wf}\right) I_r e^{-\emptyset_s/T_{eV}} \quad (7)$$

were I_i is the Bohm current at the sheath edge and I_r is the random electron flux at the sheath edge.

As the diameter of the orifice in an orifice HC decreases, the gas pressure within the cathode increases due to the presence of the orifice, leading to a gradual shift in the heating mechanism towards electron bombardment and orifice heating. Electron bombardment heating is enhanced with relatively high internal cathode pressure and discharge current; this results in decreased electron temperatures and sheath potentials. As a result, a portion of energetic electrons that possesses enough energy to surpass the sheath potential reach the insert surface, depositing their kinetic energy on the insert surface and keeping it at the thermionic emission temperature. Ion bombardment heating in the orifice cathode is mitigated simultaneously because of the reduced sheath potentials. Orifice heating is another cathode heating mechanism that dominates in the orifice cathode, commonly occurring in neutralizer cathodes. The small orifice creates high internal pressure in the orifice and insert regions. As the plasma passes through the orifice, it encounters high resistance, i.e., increased collisions between charged particles, producing significant resistive heating in the orifice plasma. This ohmic power is then convectively transferred to the orifice plate by plasma bombardment, where the energy balance is dictated by wall and Coulomb collisions [101, 102] and eventually heats the insert through conduction and radiation.

III. PLASMA INSTABILITIES IN HOLLOW CATHODE

HCs are a reliable source of high-density plasma for EP systems. Despite their effectiveness, the operation of HCs is characterized by the emergence of distinct oscillatory modes. Among these modes, the plume and spot modes have been the most extensively investigated [39, 103, 104]. Additionally, the historical literature has identified two more modes of HC operation: the diffuse mode [105-107] and the stream mode [48]. The final mode, jet mode [108], is defined by introducing neutral gas into the cathode or plume region to mitigate plasma instability [109].

The spot mode is a relatively quiescent, stable discharge mode that produces a ball or "spot" of plasma downstream of the cathode exit, while the plume mode is a precarious mode characterized by a widely diverging plasma cone extending from the cathode that fills the vacuum chamber with diffuse plasma. The transition from spot to plume mode is of great interest in studying cathode physics because it is associated with an ionization-like instability that can generate energetic ions and enhance cathode erosion [47]. The properties of this transition were initially observed during laboratory experiments of the earliest mercury ion thrusters in the late 1960s. [110], where It was observed that the luminosity of the "plume of plasma" intensified, and its characteristic size increased as the mass flow rate was lowered. [39, 103, 104].

Subsequent laboratory investigations have demonstrated that the transition is contingent upon various factors, such as the discharge current ratio to mass flow rate, the discharge current, cathode orifice size, applied magnetic field, anode geometry [81], and anode position [111]. However, because this ratio depends on several other parameters, including the cathode geometry, the transition had to be characterized empirically [47]. It is a well-established fact that in the plume mode, there is an increase in the keeper voltage oscillation and cathode orifice plate wear due to the higher production of energetic ions in the near cathode plume region, which has been observed through various studies [112, 113]. Severe degradation in the overall cathode life is caused by the sputter-erosion of external surfaces such as the keeper face and orifice plate by energetic ions.

When a HC operates in the diffuse mode, the plasma generates strong luminescence within the volume between the electrodes and throughout the entire vacuum chamber [107]. This phenomenon occurs when the flow rate is below a certain level, and the neutral gas in the chamber is excited, possibly through interaction with the wall. The diffuse mode is characterized by a low-frequency oscillation similar to the plume mode but with greater amplitude and coherence [107]. The frequency increases as the anode current increases during the transition from the plume to diffuse mode. The diffuse mode exhibits a larger plasma column radius or length, which increases the

ion temperature [106]. Figure 6 presents the photographs of the spot mode, the plume mode, and the diffuse mode.

The stream mode is a phenomenon that occurs at high gas flows, which is well above the optimal range for the spot mode in HCs [48]. In this mode, the plasma spot is pushed far downstream of the keeper orifice, and dark space is typically observed between the keeper electrode and the plasma spot. The plasma expands and disperses more rapidly in this mode than in the usual spot mode. However, very high cathode flow rates can negatively impact discharge performance in ion thrusters by suppressing the discharge voltage, which reduces the ionization rate [48]. The jet mode is a unique operational mode in HCs, especially in high-current HCs, where neutral gas is injected into the cathode or plume region to dampen plasma instability and reduce the number of high-energy ions [109]. This mode is identified by a highly collimated and stable plasma jet produced by the cathode [108], which will be discussed in Section IV.

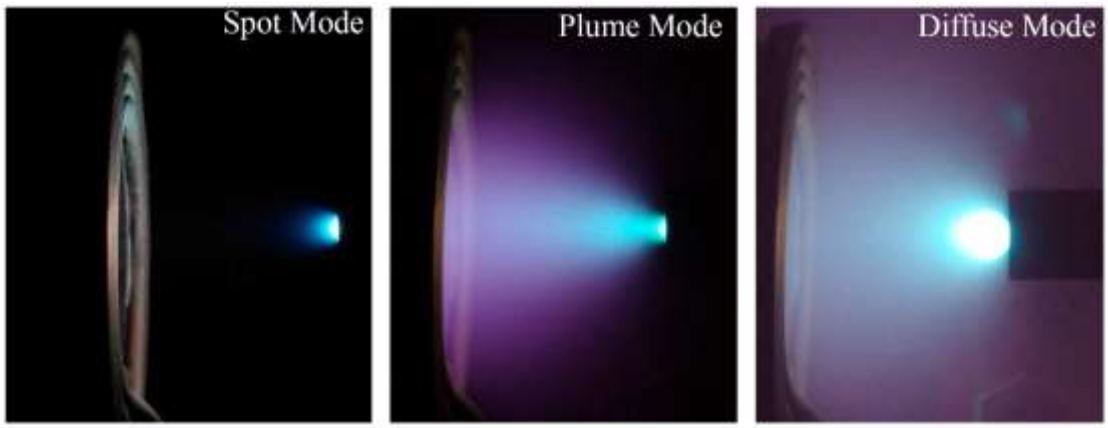

Figure 6 Photographs of the spot mode, the plume mode, and the diffuse mode [107].

Plasma oscillations in the cathode plume can be classified into three main groups based on frequency ranges [46, 47]. The first group includes power supply-induced oscillations occurring at frequencies below 1 kHz. The second group consists of coherent, large-scale oscillations occurring in the near-field plume with frequencies below 150 kHz. The third group includes broadband, turbulent fluctuations at frequencies above 200 kHz [46]. Figure 7 presents the Fourier transform of an ion saturation current probe signal. The signal analysis showed the presence of low-frequency oscillations with a peak around 100 kHz and high-frequency broadband waves above 200 kHz. The low-frequency mode corresponds to an ionization-like wave observed in plume mode, characterized by large-scale oscillations [114]. The higher-frequency modes are linked to ion-acoustic turbulence (IAT), a form of instability propagating in the plume of HCs [114]. However, the amplitude of these waves is typically less than 1% of the background density and plasma potential, and it strongly depends on the operating conditions and facility pressure [46].

Investigating IAT and ionization instability is crucial for the development of hollow cathodes. These phenomena can impact the performance and lifespan of hollow cathodes, which shows certain relations to the high-energy ion production in hollow cathode plumes [109]. Understanding and mitigating these instabilities can help optimize cathode design, extend lifespan, and enhance stability and efficiency. The following section surveys the observations made on these two oscillations.

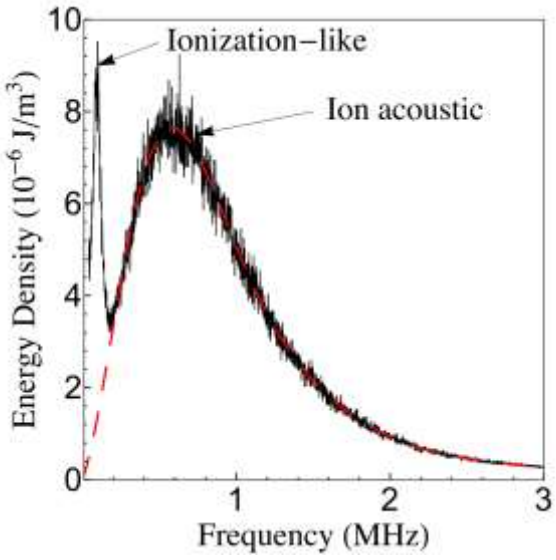

Figure 7 Fourier transform of plasma waves in a hollow cathode plume reveals ionization-like and broadband ion-acoustic waves. [114].

ION-ACOUSTIC TURBULANCE

The onset of IAT has been linked to the high-frequency plasma instability observed in HCs for propulsion [46]. The IAT is a natural phenomenon that arises in plasmas with a significant electron drift velocity and a large disparity in ion and electron temperatures. The low ion temperature and strong electron current in the HC plume make it an ideal environment for the onset of the

IAT [115], which is a collisionless process of inverse electron Landau damping that leads to non-classical ion heating [116, 117] and non-classical drag on the electron population in the cathode plume [100, 115, 118].

The IAT has been shown to exhibit low amplitude, incoherent and broadband fluctuations that can be characterized by a linear dispersion relation with a group velocity on the order of the ion sound speed [47]. The amplitudes of these waves are typically less than 1% of the background density and plasma potential but strongly depend on the operating conditions and facility pressure [119]. An increase in discharge current leads to an increase in energy of the high-frequency modes, while an increase in gas flow rate or facility pressure results in the damping of wave amplitudes through charge exchange collisions. The power spectrum of the IAT fluctuations is continuous and ranges from 200 kHz to 10 MHz, exhibiting a power decrease inversely with frequency and a cutoff at low frequency [115].

Recent developments in the modeling and experimentation of HCs have shown that the emergence of the IAT at a higher discharge current or low mass flow rate can induce coherent ionization-like instabilities [120-122], although there is no current evidence to suggest that the IAT alone can cause sputtering and cathode erosion. Georgin et al. [122] have established a clear correlation between IAT and ionization-like instabilities in cathode plume mode discharge. In the last decade, researchers have begun to investigate the impact of IAT in HCs for propulsion in greater detail. The results of experimental and numerical studies conducted in recent years have uncovered the importance of IAT in influencing the near-field plasma properties within HCs.

LARGE-SCALE IONIZATION OSCILLATIONS

Recent observations have revealed the presence of plume mode oscillations, which display quasi-coherent and longitudinal behavior at a frequency range of 10 to 150 kHz. These oscillations have three characteristics: they cause large-scale fluctuations in plasma density, plasma potential, and discharge current, with amplitudes approaching 100% of background levels [47]. Additionally, the modes are slow-moving, with dispersionless propagation or propagation at the ion drift speed from the cathode to the anode [46]. Despite the recent prevalent notion associating the plume mode oscillations with ionization instabilities [48], earlier studies have proposed several explanations to elucidate this phenomenon.

An early explanation for plume mode oscillations involves a current imbalance in the anode sheath, which occurs when the passive current to the anode is insufficient to maintain the imposed anode current [123]. A stable anode potential is formed under high mass flow rates due to the thermal electron flux generating thin electron-repelling sheaths, known as the spot mode. However, at low mass flow rates or high discharge currents, the plume mode occurs when an electron-attracting sheath forms, leading to a rise in anode potential and significant temporal variations because the lower plasma density fails to produce the necessary current. This regime also has a higher electron temperature due to the less collisional environment. Another possible cause of plume mode oscillations is ionization waves, i.e., moving striations [124-126]. These waves usually occur in DC positive column discharges and are created by a kinetic resonance between the electron energy distribution function and spatially periodic electric fields [127]. However, backward waves are typically observed in striations, which do not match the wave propagation measurements of the plume mode [128]. Besides, striations usually happen at higher pressures than the typical values found in the plume of a cathode discharge [107].

Recent studies have utilized high-speed imaging techniques as a non-intrusive diagnostic tool to directly photograph the plume mode oscillations in the cathode plume, in addition to probe-based studies [109]. This technique is commonly used to obtain information on the overall behavior of low-frequency instabilities in thrusters and cathodes [129, 130]. Georgin et al. [107, 128] and Goebel et al. [47] used a high-speed camera to capture the visual appearance of the low-frequency oscillatory modes.

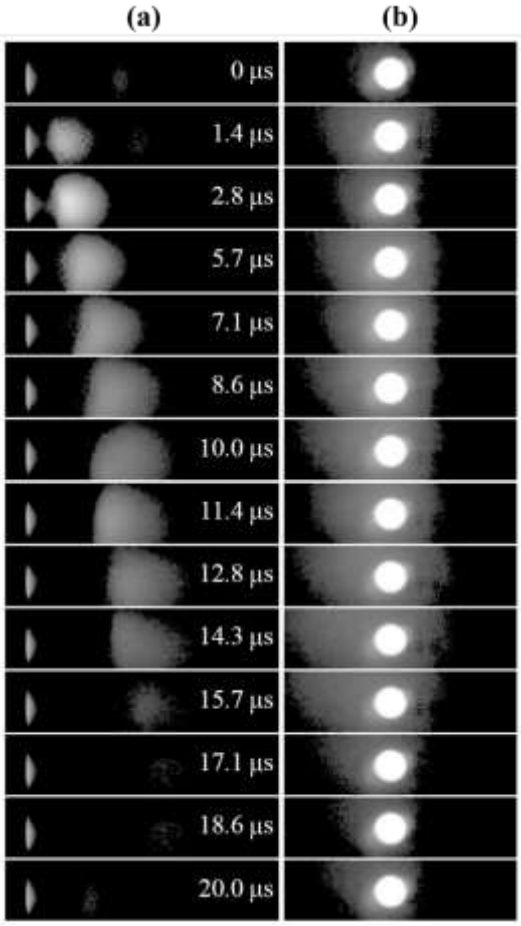

Figure 8 High-speed camera images of the plume mode instability from (a) the cathode side and (b) the cathode front [107].

Figure 8 presents a complete cycle of the plume mode instability oscillation at 20 A discharge current and 6 SCCM Xe, as captured by the high-speed camera [107].

The bright spot at the left-hand side of the image corresponds to the cathode exit, while the anode is on the right-hand side. The plume mode oscillations exhibit a cycle that repeats at the same position after about 20 μs, with a 50 kHz periodicity corresponding to previously characterized ionization instabilities [109]. The changes in light intensity observed during these oscillations are likely associated with the processes that cause the discharge current to oscillate. The ionization instabilities are known to grow when the discharge current reaches a certain threshold and when the input gas flow is reduced; this leads to a depletion of the neutral gas and a subsequent drop in the neutral density, reducing the plasma density that carries the discharge current and inducing oscillations on the ionization rate time scales [47]. Recent studies indicate that nonclassical effects such as enhanced resistivity and ohmic heating from IAT may be responsible for driving these large-scale oscillations [128, 131].

According to Goebel et al. [47], the axial burst observed through the high-speed camera resembles the characteristics of the well-known breathing mode or predator-prey ionization-instability mode of Hall thruster plumes [48, 132, 133]. Predator-prey ionization-instability is characterized as a "feast" and "famine" cycle for the electrons, in which the ionization rate is high when the neutral density is high and low when the neutral density is low. In the predator-prey model, the neutrals act as the prey and the electrons as predators. The electron density and ionization fraction increase with increasing current until a threshold is reached where the electron density becomes too high and ionizes too many neutrals. As a result, the neutral density decreases, causing the ionization rate to decrease, which leads to a subsequent decrease in the electron density [107]. This cycle of feast and famine for the electrons is a stable point in the Lotka-Volterra system of equations that describes this type of oscillation [134].

A recent study by Potrivitu et al. [135] found that the plume mode instability for the low-current operation of HCs is similar to that of high-current cathodes. The growth of IAT in the cathode plume is considered the cause of the instability. Observations show that despite the lower energy of the coherent wave and IAT in low-current cathode operation, both IAT and coherent fluctuations were present in the plume mode. These fluctuations were highly correlated, especially at higher currents, suggesting a current-driven process. During sub-ampere operation, the electron transport in the cathode plume is driven by anomalous electron collision, and the study reveals a correlation between the plume mode instability and the IAT.

Conversely, several investigations have revealed that higher field strengths in the presence of an applied magnetic field, which simulates the thruster environment, lead to a reduction in the amplitude of the ionization instability [107]; this suggests that other instabilities can arise in the plasma under these conditions. For example, the drift instability can propagate azimuthally across the magnetic field lines [107, 136, 137], and the kink instability can occur at large discharge currents [130].

IV. HOLLOW CATHODE WITH EXTERNAL HEATER

The heating of the insert in a HC is necessary to reach the thermionic emission temperature, typically accomplished through an external heater. The heater must be able to withstand high temperatures and be electrically isolated in order to heat the cathode tube via Ohmic heating. Refractory metal wires such as tungsten and tantalum are commonly used to supply the high temperatures needed for heating. However, the heater is susceptible to a range of failures, including melting, short circuits, and thermal fatigue [138, 139], and must possess the capability to endure thermal cycles of the order of 10^5 [46, 48]. Due to the critical role of the heater for cathode ignition, several types of heaters have been used, including alumina flame/plasma sprayed heaters, potted heaters, sheathed heaters, filament heaters, and radiation heaters [140-145].

The susceptibility of alumina insulation to cracking, causing heater failure, led to the supersession of the alumina flame/plasma sprayed HC heaters by other heater types. Although these heaters were successfully flight-tested [142], subsequent investigations in programs utilizing cathodes with larger diameters uncovered the propensity of the alumina insulation to develop cracks following just a few thermal cycles [143]. Additionally, the fabrication procedures involved were highly skilled and required more attention to detail than for sheathed heaters [146]. Alumina is also the material of choice for ceramic potting, used to make potted heaters. However, high-temperature exposure leads to sintering and grain growth in the alumina insulation, which could lead to void formation and short circuits [46, 145].

A common type of heater used in high-current HCs is the tantalum-sheathed alumina-insulated heater [147-149], which has a tantalum core and shield joined to create the path for the electric current.

Figure 9 Tantalum-sheathed heater on the TDU cathode [150].

Figure 9 shows the photograph of a tantalum-sheathed heater. However, this type of heater faces three problems. First, powdered alumina-insulated heaters are prone to sintering and grain growth at high temperatures,

which can cause void formation in the insulator and eventual short circuits within the heater.

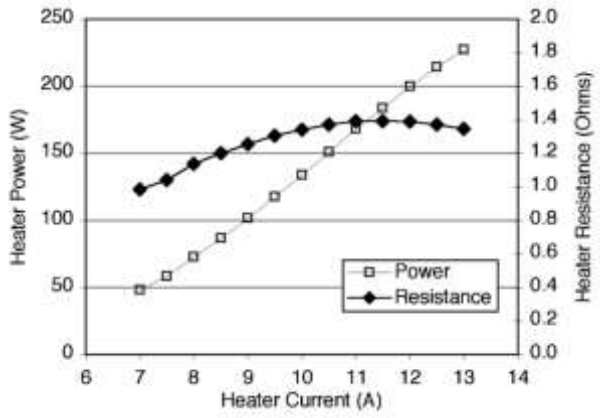

Figure 10 Heater power and resistance versus heater current [149].

Figure 10 presents the relationship between heater power and resistance concerning the heater current in a HC [149]. The findings reveal that beyond 11 A, the resistance of the cathode does not increase and even decreases at higher currents, indicating the occurrence of leakage between the center conductor and the sheath. Second, the tantalum-sheathed heater is prone to keeper shorts caused by radiation shielding or thermal expansion. Third, if the heater fails, it can be challenging to fabricate a replacement [145]. Developing higher temperature insulators to improve this type of heater's durability and duty cycles is desirable.

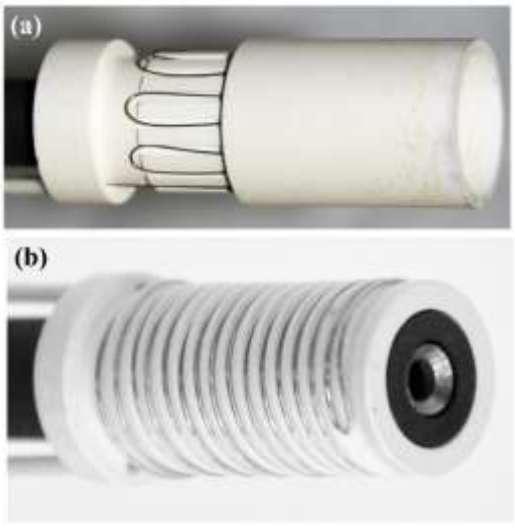

Figure 11 Filament heater windings for ceramic-encased heaters: (a) serpentine winding with the outer sleeve half-removed and (b) bifilar winding with the outer sleeve completely removed [145].

Filament heaters have been proposed as a potential option for high-current HCs, with demonstrated power capabilities in the hundreds of watts. However, careful selection of both the filament and insulation material is necessary to avoid chemical interactions or filament evaporation, which can limit their lifespan in-space propulsion applications. For instance, at elevated temperatures, the infiltration of boron into the interstices of neighboring metal matrices can cause embrittlement and fracture, as boron is present in BN. This effect is similar to the materials compatibility issues observed in LaB_6. Two examples of filament heater designs [145] are shown in Figure 11, including serpentine and bifilar windings wound on a ceramic mandrel with an insulating ceramic sleeve. Although not explicitly shown in the figure, these types of heaters have been utilized in flight ion and Hall thrusters, indicating their potential for use in higher current HCs in the future [150].

The use of radiation heaters for HCs is limited due to their low thermal transmission efficiency to the insert and susceptibility to thermal failure. Radiation heaters heat the insert primarily through thermal radiation and are commonly used in flat plate emitters or low-power HCs [80, 81, 151]. Figure 12 shows a schematic of a radiation heater in a flat disk emitter HC. While chemical reactions between the heater and insert can be mitigated, radiation heaters can only transfer a few watts of power to the insert, making them insufficient for many high-current HC applications. Additionally, overheating or thermal fatigue can cause the heater to degrade or even melt, resulting in reduced cathode performance or complete cathode failure. Therefore, radiation heaters are rarely used for HCs in space applications.

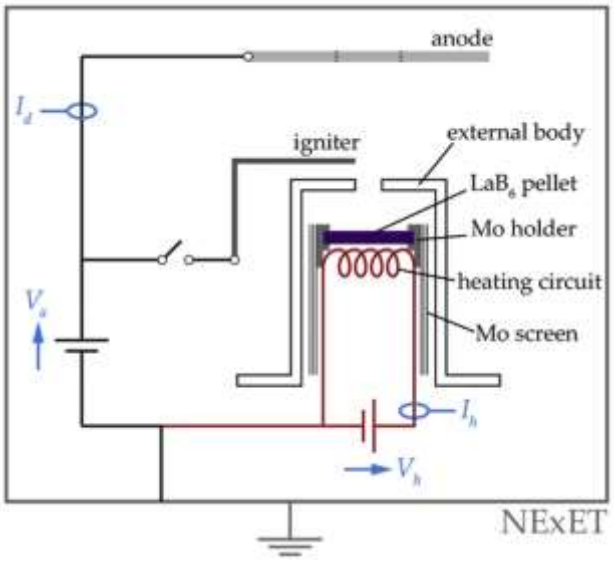

Figure 12 Schematic of a radiation heater in a flat disk emitter hollow cathode [80].

Due to the different aspects that need to be considered when designing low-discharge-current and high-discharge-current hollow cathodes, there are specific requirements for each. For example, the thermal resistance

of low-discharge-current hollow cathodes must be optimized to achieve self-heating discharge [152], while high-discharge-current hollow cathodes must avoid overheating of the emitter [153]. Therefore, the developments and considerations for these two types of hollow cathodes will be discussed separately in the following sections.

LOW-CURRENT HOLLOW CATHODE

The orifice HC with a large aspect ratio, featuring a small orifice and a large length-to-diameter aspect ratio, has been identified as an appropriate choice for low-current operation and relatively high internal gas pressure, which exploits the orifice self-heating mechanism [154, 155]. However, recent testing of several low-current cathodes has revealed a significant issue arising from the absence of a dedicated design for low-current operation. In particular, maintaining a self-sustained mode becomes difficult, necessitating an additional heater or keeper power [152]. This difficulty can be attributed to these cathodes being oversized for their respective thrusters, and specific aspects of low-current levels had not been considered [46]. Studies have suggested that impregnated barium-based insert is ideal for sub-ampere HCs. A significant benefit is that they can operate at lower temperatures than devices using LaB_6 inserts. The C12A7 electrode is being studied as a novel alternative material due to its presumed robustness and potential for further reducing operating temperatures [98, 156-158]. However, further research is required to understand the characteristics of C12A7 better and to increase its level of development to match that of conventional materials used in HCs.

Designing a low-current HC requires consideration of several aspects. First, to reduce the heat flux away from the insert region through conduction, minimizing the cathode tube's wall thickness is advisable [159]. Meanwhile, structural properties to withstand launch shock and vibration should be taken into account, in addition to manufacturing limitations, when considering the wall thickness of the cathode tube. Moreover, the cathode tube should be made from a low thermal conductivity material and be designed with a sufficient length to minimize contact with other structural components [160]. Second, low-current HCs usually possess a narrow orifice aperture to heat the insert through resistive heating in the cathode orifice [46]. However, a smaller orifice entails an increased gas pressure within the insert region, limiting the plasma contact region along the insert surface and increasing the temperature of the insert downstream end [48]; this is another aspect that needs to find a compromise between different aspect ratios and orifice heating. Lastly, since the operating temperature of a low-current cathode is typically lower than a high-current HC, the material selection for the insert must be considered during designing a low-current HC. Insert material with a higher work function, such as LaB_6 or refractory metals compared to BaO-W and C12A7, may not be able to reach its thermionic emission temperature enough for nominal low discharge current.

Puchkov et al. [161] have designed and tested a low-current cathode to minimize heat loss in the cathode body with a tungsten emitter insert impregnated with barium-calcium aluminate (BaO-CaO-Al2O3) compounds. Figure 13 presents the low-current HC in the research. The cathode was tested with varying xenon flow rates and discharge currents. The study proposed a simple method to evaluate the power released in the emitter unit and used this evaluation to develop a scheme for the emitter unit of the cathode. The cathode demonstrated stable performance with a keeper current of 0.4 A and a keeper power not exceeding 10 W.

Figure 13 Photograph of the low-current hollow cathode [161].

A HC operating at a Xenon flow rate of 0.15-0.20 mg/s and a discharge current of 1.25 A has been developed by Parakhin et al. [67] at EDB Fakel for use in a 225 W powered SPT-50 stationary plasma thruster. The cathode requires no warm-up after starting and is sustained by the discharge current. However, when switching to high-voltage modes with a decreased discharge current, using LaB_6 as an emissive material poses difficulties. Thus, a new technology was developed to manufacture barium oxide-based thermionic emitters with improved resistance to impurities generated in plasma gas. The experiments confirmed that operating at lower discharge currents and flow rates provides benefits in using a barium oxide-based emitter over lanthanum hexaboride. Stable parameters were obtained in an acceptable range of operating currents and flow rates, and no degradation was observed during 350 hours of testing.

Another LaB_6 HC, called KE-1R cathode, was developed at EDB Fakel by Saevets et al. [162], which intended to increase the specific impulse by reducing the cathode flow rate. Additional thermal screens were implemented in the cathode design to reduce heat fluxes from the emitter, which requires increased cathode time or power before starting the thruster. The cathode's position was also changed to prevent erosion of the ceramic cap of the ignition electrode. Tests were carried out to determine the optimum position of the cathode, which was mounted on a movable bracket. Meanwhile, half-caps of titanium were placed on the cathode to determine the erosion rate, as shown in Figure 14.

	Old Position	New Position
Test Duration, h	100	
Erosion Rate, mg/h	1.00	0.30
Erosion Rate of Ceramic (calculated), mkm/h	0.35	0.11
Total Sputtering time (predicted), h	4200	14000

Figure 14 Half-cups erosion at the two positions [162].

A new open-end knife-edge LaB_6 emitter HC, called the PSAC-KE cathode, has been developed by Potrivitu1et al. [42] and tested for miniaturized EP systems, particularly low-power Hall thrusters.

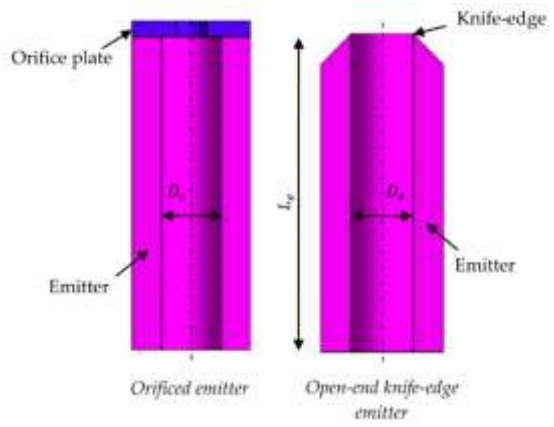

Figure 15 Schematic of the open-end knife-edge LaB_6 emitter (right) [42].

Figure 15 shows the schematic of the open-end knife-edge LaB_6 emitter. Electrostatic simulations have shown that the new cathode has an enhanced electric field within the emitter region compared to the orifice emitter PSAC cathode [152, 163]. The cathode's thermal management has also been improved based on iterative thermal simulations driven by different cathode geometries and material combinations. Tests with xenon in diode mode and triode mode have shown that the new cathode achieved ignition at low heating power below 35 W, self-sustained operation at 1 A when in standalone mode, and < 1 A when against a low-power Hall thruster. Further improvements to the cathode's thermal design, such as orifice geometry while preserving the knife-edge feature and sub-millimeter keeper orifices, may reduce the cathode's mass flow rate and promote self-sustained operation at lower emission currents.

To address the challenges faced by low-current HCs, such as discharge instabilities, narrow self-sustaining margins, and high power consumption, Li et al. [164] propose a new HC design with an additionally inserted core. The results showed that this design significantly improved the cathode's self-sustaining margin, reduced power and propellant consumption, and minimized oscillations. The study demonstrated a significant reduction in flow rate to as low as 0.07 SCCM, a lowered discharge current to 0.15-0.2A, and a decrease in power consumption to 5 W. The improved performance was due to enhanced thermionic emission on the core tip, thermally insulated from the tantalum tube, and increased thermionic emission under direct contact with the dense plasma. However, a significant issue with the core structure is its limited lifetime. The study recommends exploring alternative materials that can withstand high temperatures to address this problem. Additionally, the intrusion depth of the core into the plasma needs to be optimized to balance the benefits of the Schottky effect with the setbacks of plasma-enhanced redeposition. These optimization efforts could help to increase the longevity and stability of the proposed core structure, making it a more viable solution for low-current HC operation.

McDonald and Caruso [98] explore the potential of calcium aluminate electrode C12A7 as a low-temperature electron emitter for HC. The authors report on the initial operating characteristics of tubular C12A7 inserts in two HC configurations originally designed for a LaB_6 20A HC but operated at reduced currents of 30–150 mA. The results show that C12A7 cathodes merit further investigation and improved thermal and plasma design. The cathodes were successfully ignited with a gas pulse and low heater power, but one of the C12A7 inserts degraded due to overheating and thermal stress. The other cathode settled in at 30 mA with continuous heater power of about 30 W and later operated at 100 mA with no heater power. Although the low operating currents tested to date, the results suggest that C12A7 may be at least as strong an electron emitter as LaB_6 at moderate temperatures <1000 C. Hua et al. [165] investigated the degradation mechanism of C12A7 in low-current HC through microscopic analysis of a degraded emitter after 10 hours of thermal electron emission. Scanning electron microscopy (SEM), energy-dispersive spectroscopy (EDS), and x-ray diffraction (XRD) were used to characterize the morphology and composition of overheated electrode emitters, indicating melting and decomposition of the surface layer. The experimentally monitored temperature of the electrode emitter during operation suggests that an average current density of 64 mA/mm^2 is safe to avoid overheating. The degradation and depletion mechanisms of electrode emitters during HC operation are discussed based on experimental results and microscopic characterization and suggest that electrode degradation on the emitter surface is the cause of difficulty in cathode ignition.

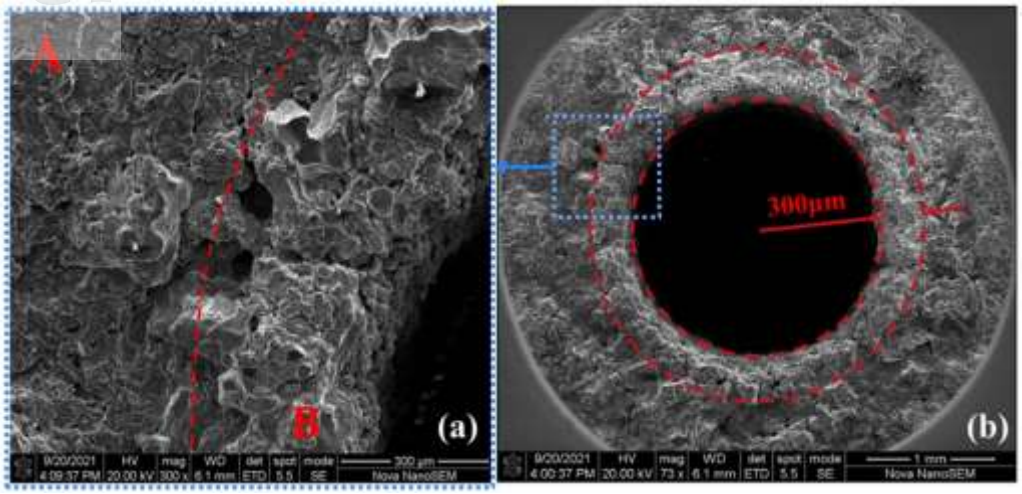

Figure 16 SEM images of the cross-section of the degraded C12A7 emitter. (a) Region A is the layer away from the insert surface, and region B is the layer close to the insert surface. (b) Ring-shaped discolored area with a width of about 300 μm [165].

Figure 16 shows the SEM images of the degraded C12A7 emitter. The results also indicate that electrode material is temperature-sensitive and easy to overheat, leading to emitter softening and deformation.

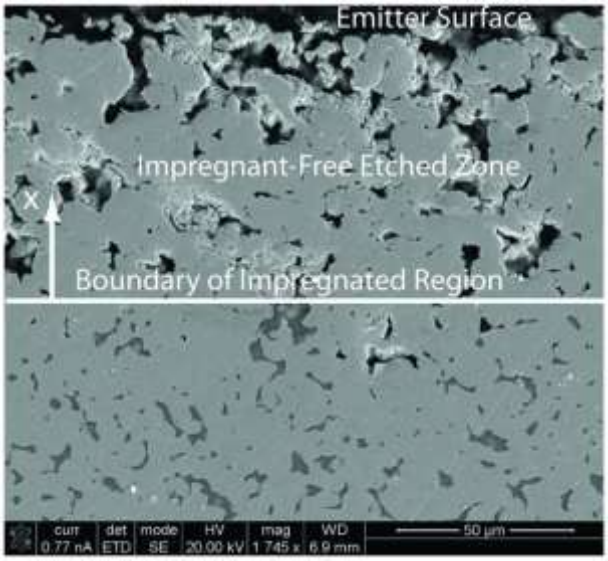

Figure 17 Photomicrograph showing pores containing impregnated material (bottom of image) and the impregnant-free etched zone near the surface (top of image) [168].

Figure 17 shows the photomicrograph of barium depletion of an insert cross-section. The surface evaporation of barium at temperatures above 1200 °C can exceed the supply rate from tungsten pores, leading to decreased surface coverage and increased work function [73, 74, 169], which is shown in Figure 3. Moreover, tungstate and tungsten crystal formation also become a significant issue at the same temperature level [170]. Controlling the temperature becomes challenging with increasing power deposition on the cathode tip region as the discharge current rises [46, 166, 171].

The severe insert degradation in the dispenser cathode makes LaB_6 an ideal candidate for high-current HC. As mentioned above, LaB_6 is a thermionic emission material with a higher work function than BaO, allowing it to operate at a higher temperature than BaO and providing enough emission current density for high-current HC operation. Meanwhile, the higher emissivity of LaB_6 compared to BaO prevents it from overheating through thermal radiation. LaB_6 is also known for its high robustness against poisoning and ability to withstand high-current densities. Due to the bulk material emission mechanism, no chemical reaction is necessary to establish a low work function surface, making LaB_6 cathodes insensitive to impurities and air exposure, which can typically destroy BaO dispenser cathodes [46]. Graphite is a commonly used material to interface with the LaB_6 insert due to its similar coefficient of thermal expansion as LaB_6, which inhibits boron diffusion into the cathode tube's support materials at high temperatures. Graphite sleeves are commonly used to interface with and contact the LaB_6 insert. These properties make LaB_6 cathodes a promising candidate for use in high-current HCs in various applications.

Second, the temperature of the insert and orifice plate is challenging to control during high-current operation. Moreover, as the propellant flow rates in high-current operation are usually higher than in low-current cathode, the cathode internal pressure increases, and the plasma-insert contact region is limited in the downstream end of the cathode tip, resulting in partial utilization of the insert surface area for electron emission [147, 172]. In this case, the downstream side of the insert is often overheated by the significant plasma bombardment, melting the insert and shortening the cathode lifespan. To investigate the thermal profile of the insert, Polk et al. [153] employed three axial thermocouples to three different wells that were drilled in the wall of the LaB_6 insert. Figure 18 shows the

three axial wells in the LaB_6 insert where thermocouples are employed.

Figure 18 Three thermocouple wells drills in the LaB_6 insert [153].

The three employed thermocouple illuminates the relationship between insert temperature, discharge current, and the mass flow rate was presented graphically in Figure 19.

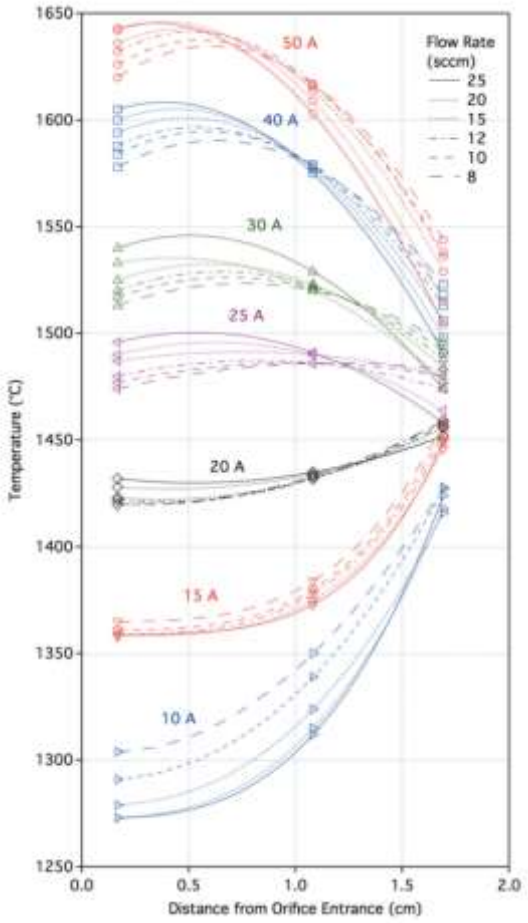

Figure 19 The relationship between insert temperature, discharge current, and mass flow rate [153].

The fitted lines in Figure 19 were included to aid in distinguishing the individual data sets and may not necessarily reflect the exact distribution between data points. The impact of mass flow rate on temperature distribution was found to depend on the level of current. Specifically, at high current levels, an increase in mass flow rate resulted in higher peak temperatures and a shift in the peak towards the downstream region.

Meanwhile, the temperature of the cathode orifice plate can exceed its nominal value because of the thermal transfer from the high-temperature insert tip through conduction and radiation. In high-current HCs, the diameter of the orifice plate is constrained due to the cathode tube and orifice being contained inside the keeper electrode, resulting in a significant issue. This constraint limits the radiated power by creating a radiation boundary. Enlarging the keeper diameter and opening the keeper orifice to the maximum extent possible without disrupting the keeper's ignition or sputter-shielding function are standard techniques to address this issue.

Last, ionization instability and IAT in the cathode plume at high discharge currents can affect the performance and lifetime of the cathode [46, 62, 79, 108, 109, 173]. Therefore, high-current HCs require additional design criteria, and instability mitigation techniques are not required for low-current HCs. In order to mitigate the ionization and current-driven instabilities observed in high-current HCs, it is necessary to develop techniques to dampen oscillations. To date, one method that has proven successful is injecting extra neutral gas in the near-cathode plume [108].

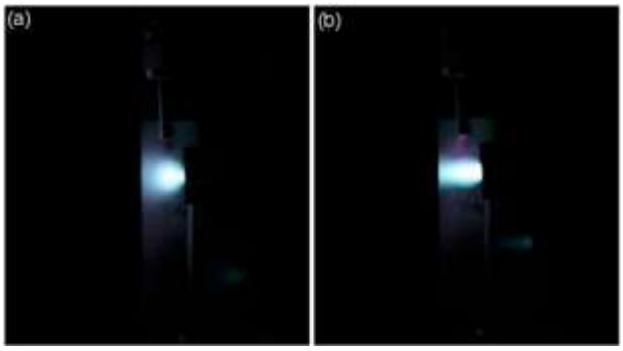

Figure 20 Photographs of the NSTAR cathode [177-179] discharge for the (a) spot-mode and (b) jet-mode case [108].

Early development of higher-current HCs was performed by Goebel et al. [78] and Tsai et al. [174] in the 1970s to achieve discharge currents of up to 800 A through a high-current HC. The main application of these devices is for non-thruster purposes, such as hydrogen ion sources for neutral beam injection heating in fusion experiments. Rawlin et al. [175] and Brophy et al. [166] developed the high-current HC for EP in the 1980s; both groups utilized the BaO dispenser cathode in high-current operation and reported insert and cathode orifice plate degradations. Friedly et al. [176] discuss the mechanism behind high erosion rates observed on downstream structures of high-current HCs in the 1990s. They postulated that a divergent jet of high-energy ions is responsible for the erosion,

which originates downstream of the cathode orifice. The mean energy and energy-spread of the jet ions both increase with the electron discharge current and cathode orifice diameter, while reductions in propellant flow rate below a threshold level also increase the jet ion energies. Goebel et al. [108] found that the plasma potential oscillation in the HC discharge caused by ionization instabilities or IAT in the near-cathode plume region can be quenched by injecting neutral gas directly into the cathode plume region near the keeper by an external gas feed and subsequently reduce the number of high energy ions [109], thereby named this the jet-mode, as shown in Figure 20.

This mode reduces the total gas flow required for the HC to run stably without plume-mode issues, which could increase the efficiency of ion and Hall thrusters by reducing neutralizer gas flow rates. The jet-mode operation can be attained by injecting gas into the plume through the keeper, but this method usually requires double the flow rate of exterior gas injection and may be influenced by the operation temperature of the cathode. Coletti et al. [180] employed several thermocouples to monitor the temperature along the insert and tested with three different orifice sizes. During operation, temperature peaks were observed at the upstream end of the dispenser and the most downstream thermocouple. The cathode lifetime was analyzed using measured data and three different criteria, showing that the cathode meets the lifetime requirement of 17,000 hours at 150A. The model used during the design phase was fitted to the data to determine necessary design changes, indicating that increasing the insert radius from 5 mm to 6 mm and the orifice radius from 4 to 4.8 mm would meet the lifetime requirement at 180A. To prevent orifice plate over-heating in the high-current cathode, in Figure 21, Becatti et al. [79] designed a 500A HC with an enlarged orifice plate with sufficient view factor to allow for radiation of deposited power in order to control the orifice plate temperature at high discharge currents.

Figure 21 The enlarged orifice plate in the 500A hollow cathode [47, 79].

A similar study has been conducted by Kamhawe et al. [181], in which three high-current cathode assemblies were tested to determine the optimal cathode configuration for meeting and surpassing the necessary discharge current and lifetime requirements of high power Hall thrusters.

Plasma penetration into the insert region is vital to provide a high contact area with the emitter and improve cathode life. The larger diameter insert was found to have significantly lower internal pressure, resulting in a longer attachment length. Plasek et al. [182] report on the experimental investigation of a large-diameter lanthanum hexaboride HC used to develop the RF-controlled HC. The effects of RF power input in the HC were simulated using a simplified two-dimensional numerical model [183, 184]. The model suggested that increasing the RF power would substantially increase the plasma density in the upstream portion of the emitter region, enhancing thermionic emission from a greater emitter area. The cathode was tested at discharge currents ranging from 20 to 225 A, and measurements were taken of cathode current-voltage characteristics and temperature profiles with varying mass flow rates and gas species. The study also identified design and operational challenges, such as high-temperature tungsten wire heaters that frequently failed due to arcing and material interactions, which led the researchers to propose using carbon wire beads as a solution. Figure 22 presents the photographs of damaged cathode components.

Figure 22 Photographs of the damaged boron nitride rings (left) and tungsten heater wire (right) [182].

Larger HCs require higher heater powers to ignite, and traditional heater designs are unsuitable for high-power operations due to material interactions and increased failure rates at high temperatures. Wordingham et al. [144] have developed a graphite heater design that can operate in the multiple-kilowatt power range and last for over 40 years of continuous operation to mitigate heater failure in high-current HC. Figure 23 shows the graphite heater utilized in the research. The team used two models, a simplified circuit model, and a finite-element model, to predict the operating temperature and resistance of the graphite heater design. The graphite heater design achieved cathode ignition and has been tested at up to 4.5 kW of heater power. The predicted 1% material loss life of the heater is over 40 years of continuous operation at 1500 °C, suggesting that the operational life provided by the graphite heater might be the candidate for high-power EP. Overall, developing high-current HCs requires a deep

understanding of the complex plasma collective behavior involved in cathode operation and careful design and optimization to achieve stable and reliable performance at high discharge currents.

Figure 23 The graphite heater with 4 pseudo-coils [144].

V. HEATERLESS HOLLOW CATHODE

HHCs are a novel type of HC that has gained interest in recent years. In this design, the cathode insert is heated to its thermionic temperature through plasma discharge without needing an external heater, which is required for conventional cathodes [185]; this is achieved through plasma discharge breakdown between the keeper and cathode tube, directly heating the insert and cathode tube tip. Once the insert has reached its thermionic emission temperature, it can sustain the primary discharge with the anode. At this point, the HHC can function similarly to a classic HC that utilizes an external heater [46, 186]. **Figure 24** presents the photograph and schematic of a low-current HHC. Since HHCs do not utilize an external heater, they offer several advantages and are a promising alternative to conventional external heated cathodes. One of the main benefits is the elimination of cathode heaters, which can be prone to failure due to thermal fatigue [139, 187]. By removing this potential single-point failure, HHCs increase the reliability of electrical propulsion systems.

Another advantage of HHCs is the reduced time required for ignition. In conventional HCs, the heating process is indirect and can take minutes or even hours to reach steady-state operation [189-191]. In contrast, the plasma discharge generated in heaterless ignition directly heats the cathode tube and insert, allowing the operating temperature to reach in seconds [192, 193]. Some HHCs have even demonstrated an immediate ignition process called an instant start [94]. Eliminating external heating elements also resulted in lower mass and reduced keeper diameter for HHCs. Additionally, the heater module in the power processing unit (PPU) for conventional HCs can be eliminated, reducing the volume, mass, and complexity of the PPU [46]. However, it should be noted that higher voltage isolation is required in the keeper supply for HHCs due to the higher voltages needed to start the Paschen discharge used for ignition [194].

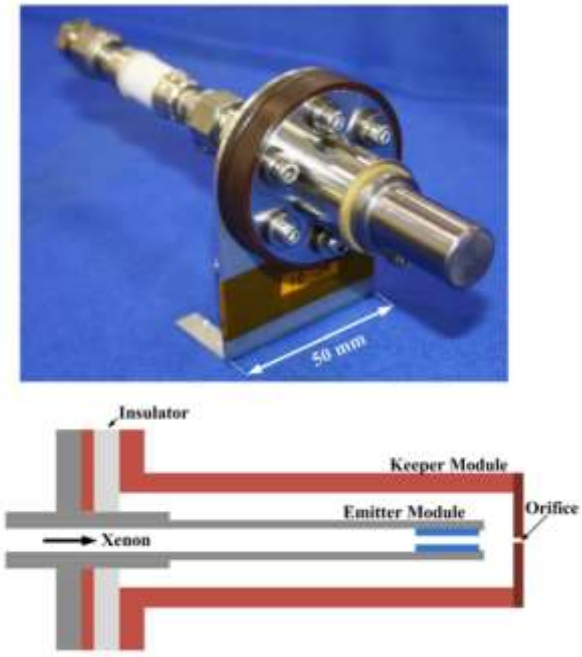

Figure 24 Photograph (top) and Schematic (bottom) of the ARC-1A low current heaterless hollow cathode [188].

HHCs are considered advantageous for EP but have limitations restricting their use in flight programs. Firstly, plasma discharge initiation at room temperature or below requires high voltages of several hundred to thousands of volts, and a high propellant mass flow rate is necessary to increase the pressure in the cathode-keeper gap [195, 196]. Consequently, the bulky nature of high-voltage ignition power modules and mass flow controllers presents a challenge to the utilization of HHCs. The ignition power supplies must contain insulating material to prevent internal breakdown, which can increase their size and mass, and the mass flow controllers must be capable of handling higher flow rates.

Secondly, conventional dispenser cathodes that use a heater are gradually conditioned by increasing the temperature, allowing impurities to diffuse out of the cathode surfaces slowly. Since heaterless cathodes lack a heater, non-conventional cathode conditioning procedures, such as using a low-power plasma discharge, must be employed to condition dispenser cathodes [197]. Thirdly, it is essential to ensure that the plasma heating of the thermionic insert achieves its operating temperature while minimizing the heat flux to other internal components of the cathode [198, 199]. Finally, the potential transition of heaterless ignitions into cathode arcing can result in significant damage to the cathode electrodes, ultimately limiting the number of ignitions and reducing the overall lifespan of the cathode, as shown in Figure 25.

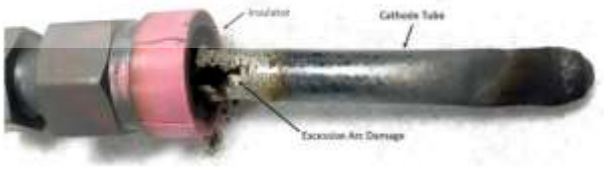

Figure 25 Discharge activity near an electrical isolator could be attributed to triple junction effects [200].

PLASMA IGNITION PROCESS

The ignition process of HHC is generally divided into three phases: initial breakdown, heating phase, and transition to primary discharge [46, 192].

In the first phase, the plasma breakdown [201] occurs between the cathode tube and the keeper. This stage aims to generate plasma to heat the insert, and ignition is usually initiated by flowing a relatively large amount of propellant gas compared to steady-state operation through the cathode, which increases the local pressure between the cathode and keeper electrode. Subsequently, a high voltage is applied between the two electrodes to initiate a plasma breakdown [195]. Many studies on HHCs have identified the optimal breakdown as the minimum point of the Paschen curve for the relevant gas. Paschen's law [202] states that the pressure between the ignition electrodes determines the breakdown voltage in a planar electrode configuration, the distance between them, and the materials used for the electrodes. Although a Paschen-like breakdown voltage behavior was present in many studies, several researchers have shown that gas breakdown may occur under voltage below the minimum predicted by the Paschen mode [203-206]. This phenomenon can be explained by the "breakdown pendulum effect" due to the axisymmetry of the HC, where high-energy electrons bounce between the electrode walls while enhancing the ionization avalanche effect [195].

The sensitivity of the breakdown voltage to specific geometry alterations, particularly sharp edges in the electrodes, has been extensively studied. In a recent investigation, Daykin-Iliopoulos et al. [196] explored the effect of detailed geometry modifications on the breakdown voltage of the HHC, as shown in **Figure 26**. The radius of curvature on the keeper orifice was reduced to increase the electric field strength, resulting in a sharp keeper orifice. The sharp keeper orifice was tested with the sharp edge facing the cathode and then reversed so that the sharp edge faced away from the cathode. The results showed that the modification significantly influenced the breakdown voltage at lower flow rates. For a flow rate of 2 SCCM, the sharp keeper orifice reduce the mean breakdown voltage by 20 percent compared to the original keeper orifice. Three different cathode orifices were also designed and manufactured, with varying inner diameters and geometries. The breakdown voltage was found to be lowest for the 1.5 mm cathode orifice at each flow rate, while the sharp geometry orifice yielded a 20 to 30 V lower breakdown voltage for flow rates above 3 SCCM. However, the impact of sharp electrodes was noted in the regime of low pressure-distance, which is considerably far from the Paschen minimum. This ignition regime has limited relevance as HHCs are generally intended to initiate near the minimum voltage required, where the impact of electrode sharpness is insignificant [46].

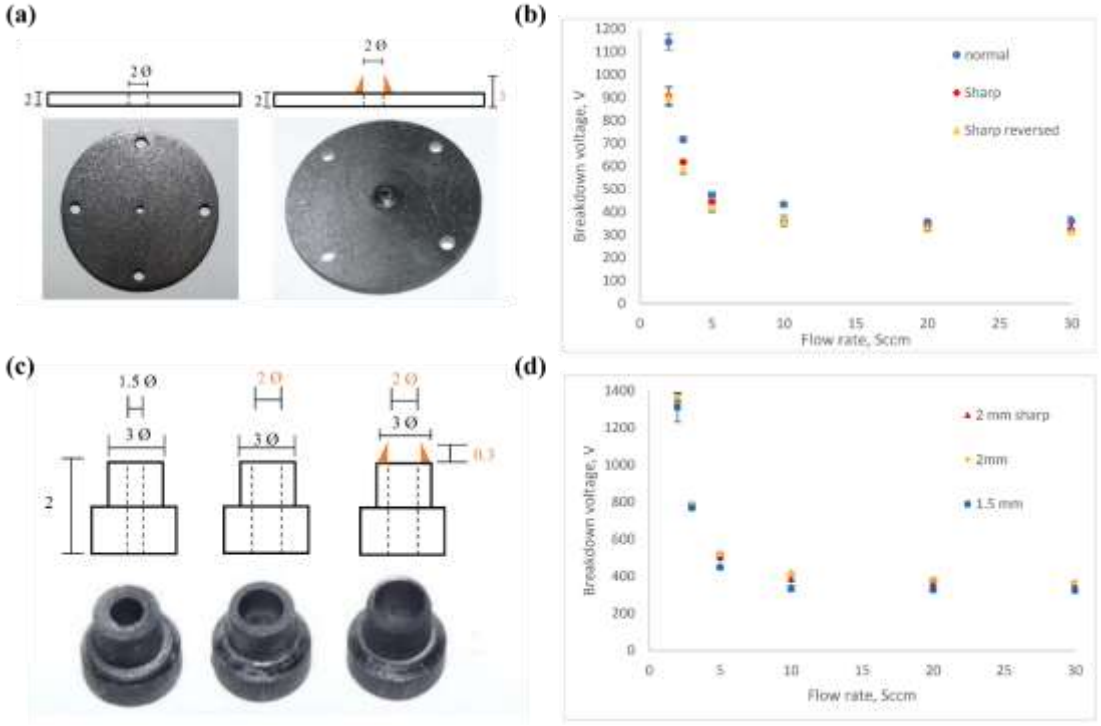

Figure 26 Schematic and geometry of the (a) keepers and (c) cathode orifices used by Daykin-Iliopoulos et al., dimensions in mm. Breakdown voltage variation with (b) keeper orifice modification and (d) cathode orifice [196].

The fix-volume release technique, also known as the pulse flow technique, is commonly used to achieve high pressure for initial plasma breakdown in a HHC [200, 206-208]. This method involves injecting propellant into the cathode gas supply tube while keeping the valve at the cathode inlet closed. The pressure within the gas supply tube increases until it reaches a sufficiently high level, at which point the valve is opened, allowing gas to flow into the cathode cavity and between the ignition electrodes that are already under voltage. The local pressure in the ignition electrodes' gap peaks within milliseconds and quickly decreases until an equilibrium pressure is reached. This decrease in pressure in the inner electrode gap effectively sweeps across different pressure values, facilitating breakdown at relatively low voltage [185].

The second phase of plasma discharge in a cathode ends when the emitter is heated sufficiently to reach thermionic emission temperatures for the primary discharge. Figure 27 presents the photograph of the discharge between the emitter and keeper during the cathode heating. The images from **Figure 27** (a) to (d) are presented chronologically. After plasma breakdown, two types of discharge may occur, arc discharge or glow discharge, depending on the current limitation. In general, arc discharges are characterized by currents in several to tens of amperes and voltages in the tens of volts, while glow discharges are characterized by currents in the milliampere range and voltages in the few hundred volts [209]. During the arc discharge process, a small portion of the surface experiences a localized discharge that can result in extremely high temperatures. The high current arc discharge process provides the advantage of quickly heating the cathode. However, since the insert remains cold after breakdown, the generated arc may attach to any conductive material at the cathode potential, including the cathode structure or emitter [185]. Moreover, over-heating or extreme heating at a single point may lead to high thermal stress and fast cathode degradation [97, 98, 210].

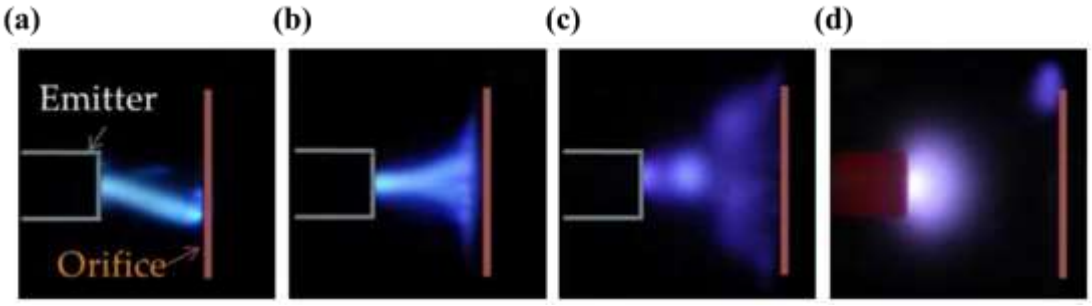

Figure 27 Photographs of (a) the beginning of the heating phase, (b) the discharge redistributes and becomes symmetrical with channel spreading towards the orifice plate, (c) the luminosity decreases and becomes diffuse with wider plasma channel diameter near the orifice plate, and (d) the thermionic emission current increase because of the heated insert [192].

Several studies have achieved Cathode heating through glow discharge [192, 195, 203, 206], which is sustained by field and secondary electron emissions [198, 207]. Compared to arc discharge, glow discharge usually results in longer heating durations, typically tens of seconds [192, 195, 206]. After the heating process, whether through arc or glow discharge, the discharge transitions to the third phase consisting of thermionic emission and steady-state plasma discharge operation. During this phase, the emitter can supply the required discharge current through a relatively large area. At this point, the gas mass flow can be reduced to the nominal value, and the discharge current can be increased by applying the main discharge power [185, 194].

LOW-CURRENT HEATERLESS HOLLOW CATHODE

The development of HHCs has become increasingly attractive for low-power EP systems due to their small size, lack of a heater, and associated power supply. However, the durability of HHCs requires further investigation. Lev et al. [211] conducted an endurance test for the Rafael Heaterless Hollow Cathode (RHHC), a low-current HC designed for operation with low-power Hall and ion thrusters. The cathode was operated in diode mode at a discharge current of 0.8 A and xenon mass flow rate of 2.5 SCCM for over 5,000 hours, during which floating keeper voltage, ignition voltage, and cathode body temperatures were monitored. The ignition voltage was consistently below 400 V throughout the experiment, and the cathode body temperature was up to 300°C initially but decreased slowly to about 250°C after 5,000 h. The results showed that the floating keeper voltage gradually decreased from 14 V to 8.5 V, which could be attributed to either improved cathode cleanliness or erosion of the keeper orifice. Gradual expansion of the keeper orifice diameter may result in lower plasma power losses in the orifice channel, which is supported by the fact that the cathode pressure also gradually decreased during the endurance test. However, post-test examination shows that the keeper orifice shape and diameter remained unchanged and revealed that the orifice plate texture became grainy-like, typical behavior of heated refractory metal parts, as shown in Figure 28. Nonetheless, Lev et al. speculated that the erosion might have occurred at the internal orifice despite the absence of external erosion, which required further examination.

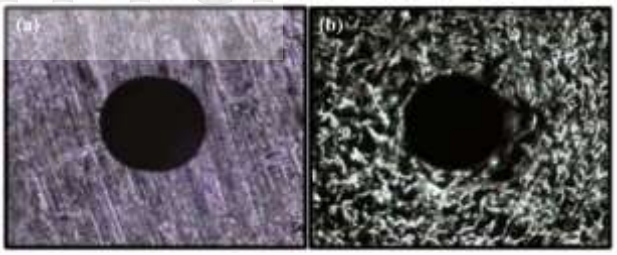

Figure 28 Microfocus photograph of the keeper orifice (a) before and (b) after the endurance test [211].

To investigate cathode degradation during ignition, Becatti et al. [194] developed a low-current LaB_6 HHC, a part of JPL's Ascendant Sub-kW Transcelestial Electric Propulsion System (ASTRAEUS). In order to understand the life and performance implications of repeated heaterless ignitions, an ignition cycling test was conducted. The cathode demonstrated more than 25,000 heaterless ignitions with no significant degradation in the steady-state operation performance. Although the time required to reach steady-state discharge increased by 2 to 3 sec after approximately 18,000 ignitions, the post-test analysis revealed slight modifications of the cathode interior and exterior surface. Figure 29 presents the post-test photograph of the cathode orifice plate with radiation shielding. The shielding elements remain pristine, and the graphite deposits at the periphery of the orifice from the keeper's surface. The achievement of more than 25,000 heaterless ignitions was attributed by Becatti et al. to three key elements: highly effective thermal isolation, a high aspect ratio keeper orifice, and a novel emitter geometry localized much of the Paschen/glow discharge heating directly to the insert.

Figure 29 Post-test photograph of the cathode after keeper removal [194].

The long-duration wear test of the ASTRAEUS cathode was conducted by Conversano et al. [40]. Throughout the test, the cathode was operated using xenon propellant at a discharge current of 4 A for 13,011 hours, during which a total of 1653 ignitions were performed. The discharge voltage had a mean value of 23.3 V with a variation of ±1 V. The peak-to-peak variation was measured at 4.19 V, corresponding to 18% of the mean value. Additionally, the discharge voltage varied by a maximum of +1.61 V/− 1.39 V from the mean value. A keeper-to-cathode short occurred during the test, which caused the keeper potential to be nearly 0 V, but it was cleared by applying a 3 A current on the keeper, and the keeper-to-cathode short did not affect the cathode discharge voltage. The cause of the short was traced to a failed weld on the tantalum radiation shielding.

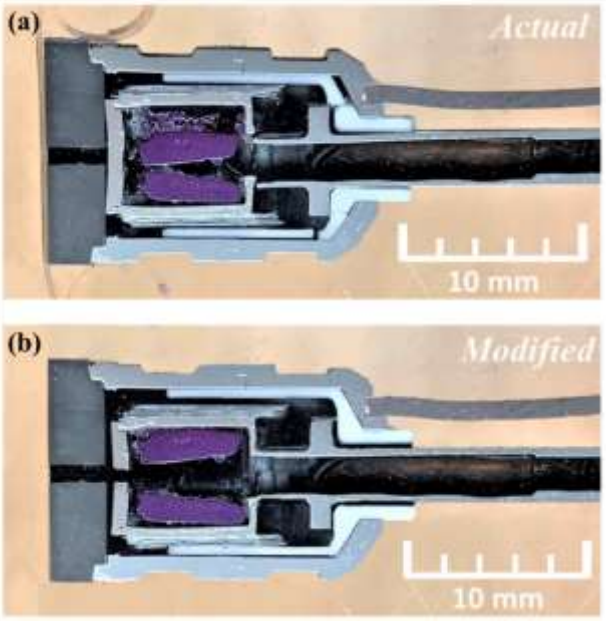

Figure 30 Post-test photograph of the ASTRAEUS cathode cross-section showed (a) the damage caused during the resin-setting and cross-sectioning process and (b) the reconstruction to better visualize the cathode's configuration [40].

Figure 30 shows the photograph of the cross-section cathode in the post-test examination. The estimated lifetime was >26,000 hours based on the evaporation of the thermionic emitter, exceeding the initial modeling predictions of 18,000 hours, which indicated that the cathode is no longer a life-limiting factor for deep-space missions using ASTRAEUS.

HIGH-CURRENT HEATERLESS HOLLOW CATHODE

The increasing demand for higher power in-space propulsion systems due to increased mission demands and payload requirements has led to the development and utilizing higher current cathodes. However, high-current HCs have not been able to demonstrate reliable heaterless ignition due to the severe erosion of the cathode orifice plate or insert caused by the formation of anchored arc spots [194].

The development and testing of a high-current HHC have been reported by Daykin-Iliopoulos et al. [212, 213],

demonstrating successful operation up to 30 A. **Figure 31** presents the schematic of the UoS 30 A LaB_6 HHC. The cathode design eliminates the need for excessive ignition voltages or propellant pulsing by utilizing a reduced keeper orifice that allows ignition with voltages below 400 V and nominal flow rates below 15 SCCM. After the cathode was ignited and thermionically emitting with the keeper discharge between 1-2 A, the discharge was maintained for a stabilization period of 1-3 minutes before applying the anode potential, with the anode current initially limited to 0.5 A and gradually ramped up to the required setpoints to support discharge stability. Once the anode discharge exceeds 1 A, the keeper discharge is switched off and left floating.

The UoS cathode shows a negative-impedance I-V discharge profile during the steady-state discharge from 1-30 A, indicating a decrease in discharge resistance while the discharge current increases. This behavior is believed to be due to sufficient insert heating through ion bombardment. The discharge I-V curve of the UoS cathode is similar to that of conventional HCs with external heaters, indicating that the UoS cathode design modifications do not significantly impact performance. Due to the thermal balance, the discharge voltage slightly varies with increasing current from 20 to 30 A. The performance of the UoS cathode has been characterized with xenon, krypton, and argon. The emitter tip temperature of an UoS cathode has been measured for the first time using optical pyrometry, and optical emission spectroscopy has been used to investigate the internal cathode-keeper plasma and determine plasma electron density.

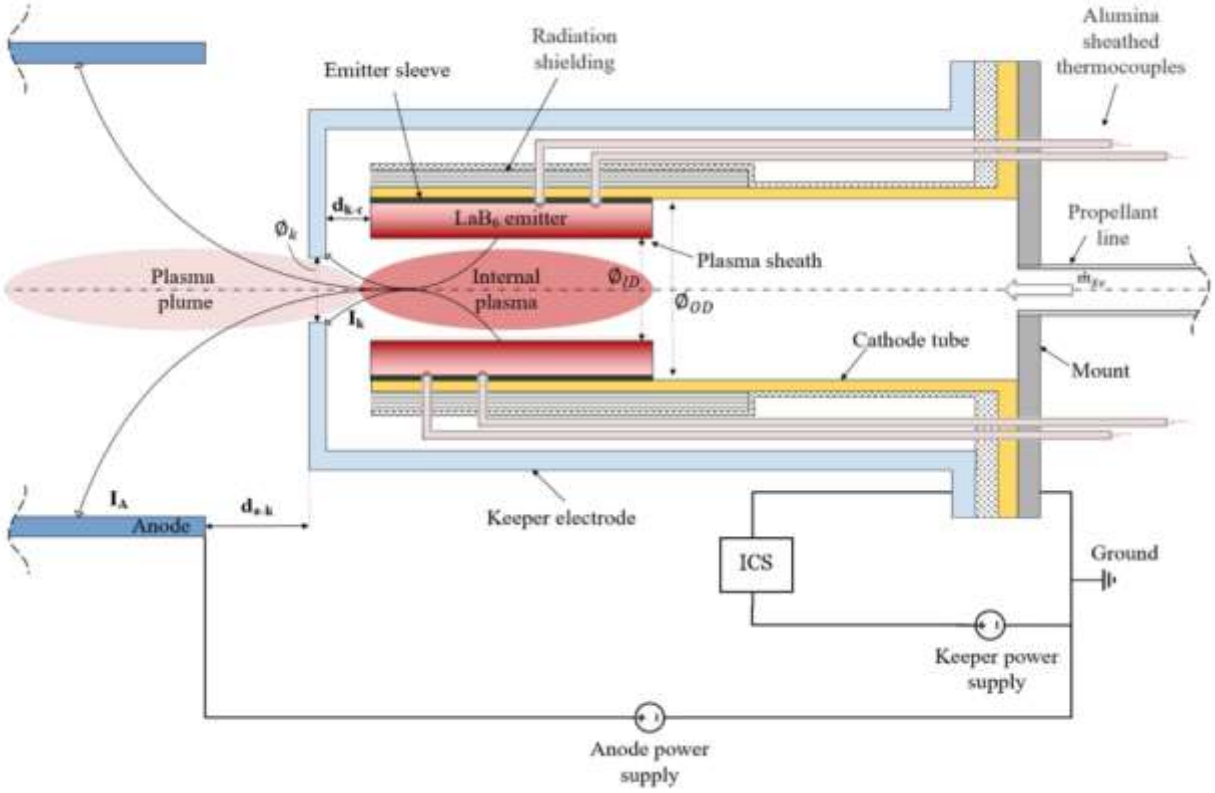

Figure 31 The schematic of the UoS LaB_6 heaterless hollow cathode [212, 213].

A higher discharge current level of 100 A has been achieved by Kojima et al. [214], which investigated the operation characteristics and plasma diagnostics of a 100 A class HHC. The study suggested that the observed unstable cathode plume was caused by forced electron extraction by the anode due to the high discharge current and ionization voltage.

To address the limitation of heaterless ignition of the high-current cathode, Goebel and Payman [44, 45] proposed a new HHC design, which utilized the tendency of lower pressure, long-path-length Paschen discharge to couple directly to the gas feed line without arcing, and named this novel design High Emission Current Cathode with Tube-Radiator (HECCTR), as shown in Figure 32.

This cathode configuration features a tantalum gas feed tube, i.e., tube radiator, at cathode potential that extends partway into the emitting insert region of the cathode. Tantalum is selected for gas feed tube material with a low evaporation rate at high temperatures. A high-voltage Paschen discharge is struck from the tube to the keeper, which heats the tube tip and efficiently radiates heat to the insert surface. The HECCTR design offers multiple advantages over traditional HHC designs. Firstly, using tantalum in the HECCTR is more robust than the LaB_6 insert, enabling it to sustain micro arcing during conditioning without damage. Secondly, the direct heating of the inner surface responsible for thermionic emission minimizes power losses to the keeper electrode and other cathode components. Finally, experimental results indicate

that the discharge spends minimal time in the Paschen regime [215], reducing the significance of the high voltage discharge's sputtering and arcing erosion mechanisms. These findings suggest that the HECCTR design offers significant benefits over traditional heaterless designs, improving the performance and reliability of high-power EP systems [44].

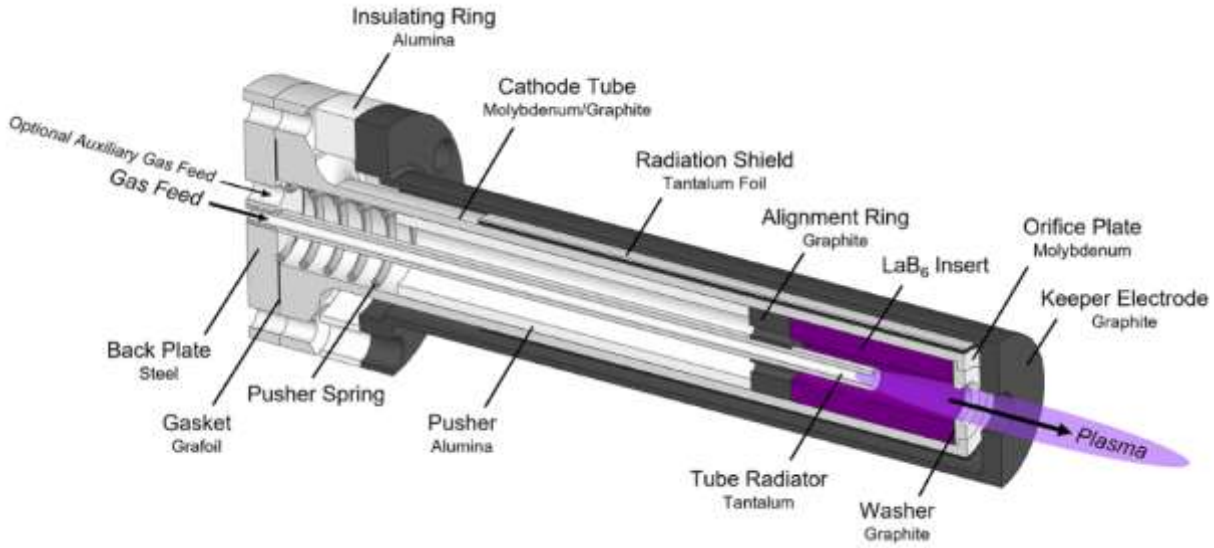

Figure 32 Schematic of HECCTR design [44, 45].

Since the extended gas supply tube in the insert region may alter the plasma structure and plasma sheath, Payman and Goebel [44] compared the anode discharge voltage versus current of the 50 A HECCTR cathode and the original TDU cathode [147, 216], where the 50 A HECCTR cathode was developed by removing the external heater element of the TDU cathode and installing a tantalum tube. The I-V curves substantiate that the plasma structure in the cathode or the emission properties of the inset did not significantly alter by the presence of the tube radiator at the insert region. Meanwhile, the calculated sheath thickness at the insert region of the HECCTR cathode (0.86 μm) is significantly less than the distance between the inner insert surface and the tube (1.6 mm). Furthermore, the steady-state discharge properties of the HECCTR cathode were found to be unaffected by its startup method, as demonstrated by the results of re-installing the TDU heater on the cathode. Finally, the results of the study revealed that the refractory metal tube's evaporation and sputtering during the heating phase were negligible and did not affect the thermionic insert's emission capabilities or properties.

Extending the 50 A HECCTR cathode design, Goebel and Payman [45] demonstrated a 300 A class version of tube-radiator heaterless cathode by modifying the X3 cathode [217, 218] into a heaterless design. However, a significant issue has been identified in the pursuit of scaling the HECCTR design to larger, high-current cathodes. It has been observed that the keeper ignition and heating power are inadequate in sustaining the cathode in a self-heating mode before initiating the anode discharge. This issue has been addressed by increasing the keeper discharge current from 6 A to 10 A with the help of an additional power supply. The lifetime prediction of the tantalum tube radiator, using the same methodology as in their previous work [44], indicates that the HECCTR design scales effectively to very high current cathodes, with the potential for many thousands of ignition cycles.

VI. CONCLUSIONS

This paper reviews plasma discharge in HC and recent advancements in HC technology. The discussion begins with thermionic emission theory and the materials used as emitters, followed by an examination of HC's self-heating mechanisms determined by various factors such as cathode geometry and internal gas pressure. Plasma instabilities in HC plumes, including the transition from spot to plume mode and ionization-like instabilities, are also discussed. This review introduces two types of HCs: the classic configuration with an external heater and the heaterless hollow cathode (HHC). For low-current HCs, the orifice HC with a large aspect ratio has been identified as suitable, but maintaining a self-sustained mode has proven challenging. Meanwhile, high-current HCs face difficulties in temperature control and ionization instability, which can affect performance and lifetime, highlighting the need for further research into these areas to address the existing challenges.

HC technology is rapidly advancing, with numerous novel developments immediately applied in industrial and space applications. Future challenges for HCs include developing a low work function material that is chemically stable to sustain propellant impurities and has a low evaporation rate with a longer lifespan. Optimizing the HC

design and further investigating plume mode oscillation to minimize high energy ion yield and mitigate cathode erosion are also necessary. Additionally, until fully predictive design codes are available, it is necessary to continue modeling cathode operation, thermal performance, and plasma discharge instabilities.

REFERENCES

[1] Choueiri EY, "A critical history of electric propulsion: The first 50 years (1906-1956)," *Journal of Propulsion and Power*, Vol. 20, 2004, pp. 193-203.

[2] Sovey JS, Rawlin VK, Patterson MJ, "Ion Propulsion Development Projects in U.S.: Space Electric Rocket Test I to Deep Space 1," *Journal of Propulsion and Power*, Vol. 17, 2001, pp. 517-526.

[3] Krestina AV, Tkachenko IS, "Efficiency assessment of the deorbiting systems for small satellite," *Journal of Aeronautics, Astronautics and Aviation*, Vol. 54, 2022, pp. 227-239.

[4] Zhang S, Yang J, He J, Li C, Wang E, Xu S, Zhang F, "A Review on the Construction Mechanism of Space Solar Power Station Network," *Journal of Aeronautics, Astronautics and Aviation*, Vol. 55, 2023, pp. 315-334.

[5] Sedelnikov A, "Algorithm for Restoring Information of Current from Solar Panels of a Small Satellite Prototype "Aist" with Help of Normality Conditions," *Journal of Aeronautics, Astronautics and Aviation*, Vol. 54, 2022, 2022, pp. 67-75.

[6] Hsiao FY, Chou WT, Cato T, Rebelo C, "Coarse Sun Acquisition for Micro Satellites Using only Sun Sensors," *Journal of Aeronautics, Astronautics and Aviation*, Vol. 53, 2021, pp. 95-104.

[7] Wang HY, Juang JC, "An Improved Precise Point Positioning Method Based on Between-Satellite Single-Difference and Carrier Smoothing," *Journal of Aeronautics, Astronautics and Aviation*, Vol. 52, No. 4, 2020, pp. 387-402.

[8] Liu X, Zhan X, Wang S, Zhai Y, "Measurement-Domain Cooperative Navigation for Multi-UAV Systems Augmented by Relative Positions," *Journal of Aeronautics, Astronautics and Aviation*, Vol. 52, 2020, pp. 403-416.

[9] Wu HY, Liao KC, Wen HT, "An Analytic Study on Mathematical Modeling of Area-Pressure Relation of Jet Engine Convergent-Divergent Nozzles," *Journal of Aeronautics, Astronautics and Aviation*, Vol. 55, 2023, pp.277-287.

[10] Wallner LE, Czika Jr J, "Arc-jet thrustor for space propulsion," National Aeronautics and Space Administration Cleveland OH Lewis Research Center, 1965.

[11] Li YH, Huang TY, Shen MM, Chen YC, "Development of Miniature Radio Frequency Ion Thruster with Inductively Coupled Plasma Source," *Journal of Aeronautics, Astronautics and Aviation*, Vol. 55, 2023, pp.13-28.

[12] Li YH, Chen YC, Liu SW, Aslan AR, "Prediction and optimization of thrust performance from plasma diagnostics in the inductively coupled plasma of an RF ion thruster," *Acta Astronautica*, 2023.

[13] Wilbur PJ, Rawlin VK, Beattie J, "Ion thruster development trends and status in the United States," *Journal of Propulsion and Power*, Vol. 14, 1998, pp. 708-715.

[14] MYERS R, LAPOINTE M, MANTENIEKS M, "MPD thruster technology," Conference on Advanced SEI Technologies, 1991, pp. 3568.

[15] Kodys A, Choueiri E, "A critical review of the state-of-the-art in the performance of applied-field magnetoplasmadynamic thrusters," 41st AIAA/ASME/SAE/ASEE Joint Propulsion Conference & Exhibit, 2005, pp. 4247.

[16] Hsieh JH, Li YH, Shen MM, Lien WC, Lin PH, "Hectowatt-Class Double-Peaked Hall Thruster for Future Space Missions," 2022.

[17] Boeuf JP, "Tutorial: Physics and modeling of Hall thrusters," *Journal of Applied Physics*, 121 (2017) 011101.

[18] Conversano RW, Goebel DM, Hofer RR, Mikellides IG, Wirz RE, "erformance analysis of a low-power magnetically shielded Hall thruster: Experiments," *Journal of Propulsion and Power*, Vol. 33, 2017, pp. 975-983.

[19] Vaudolon J, Mazouffre S, Hénaux C, Harribey D, Rossi A, "Optimization of a wall-less Hall thruster," *Applied Physics Letters*, 107 (2015) 174103.

[20] Takahashi K, "Helicon-type radiofrequency plasma thrusters and magnetic plasma nozzles," *Reviews of Modern Plasma Physics*, 3 (2019) 3.

[21] Marcuccio S, Genovese A, Andrenucci M, "Experimental performance of field emission microthrusters," *Journal of Propulsion and Power*, Vol. 14, 1998, pp. 774-781.

[22] Tajmar M, Genovese A, Steiger W, "Indium field emission electric propulsion microthruster experimental characterization," *Journal of Propulsion and Power*, Vol. 20, 2004, pp. 211-218.

[23] Li YH, Pan JY, Herdrich G, "Design and demonstration of micro-scale vacuum cathode arc thruster with inductive energy storage circuit," *Acta Astronautica*, Vol. 172, 2020, pp. 33-46.

[24] Li YH, Palagiri S, Chang PY, Montag C, Herdrich G, "Plasma Behavior in a Solid-Fed Pulsed Plasma Thruster," *Journal of Aeronautics, Astronautics and Aviation*, Vol. 51, 2019, pp. 31-42.

[25] Li YH, Dorn K, Hsieh HC, Kuo TC, Hsu YC, "Effect of Electrode Angle on Pulsed Plasma Thruster Performance," *Journal of Aeronautics, Astronautics and Aviation*, Vol. 53, 2021, pp.353-367.

[26] Wang S, Zhan X, Zhai Y, Chi C, Liu X, "Ensuring high navigation integrity for urban air mobility using tightly coupled GNSS/INS system," *Journal of Aeronautics, Astronautics and Aviation*, Vol. 52, 2020, pp. 429-442.

[27] Yahya NA, Varatharajoo R, Harithuddin A, "Satellite Formation Flying Relative Geodesic and Latitudinal Error Measures," *Journal of Aeronautics, Astronautics and Aviation*, Vol. 52, 2020, pp. 83-93.

[28] Lin CL, Tsai JR, "Preface to the Special Issue: FORMOSAT-7 Mission and Its Applications," *Journal of Aeronautics, Astronautics and Aviation*, Vol. 50, 2018, i-i.
[29] Chu CH, Fong CJ, Xia-Serafino W, Shiau A, Taylor M, Chang MS, Chen WJ, Liu TY, Liu NC, Martins B, "An era of constellation observation-FORMOSAT-3/COSMIC and FORMOSAT-7/COSMIC-2," *Journal of Aeronautics, Astronautics and Aviation*, Vol. 50, 2018, pp. 335-346.
[30] Tsai YF, Lin CT, Juang JC, "Taiwan's GNSS reflectometry mission-The FORMOSAT-7 reflectometry (FS-7R) mission," *Journal of Aeronautics, Astronautics and Aviation*, Vol. 50, 2018, pp. 391-403.
[31] Yang M, Chu FY, Lin CY, "GNSS ambiguity resolution in kinematic positioning: benefits of satellite availability and sampling rate," *Journal of Aeronautics, Astronautics and Aviation, Series A*, Vol. 50, 2018.
[32] Zhou Y, Wu PL, Li XX, "XANV/GNSS-Based Integrated Navigation Using a Robust Filtering Algorithm," *Journal of Aeronautics, Astronautics and Aviation*, Vol. 48, 2016, pp. 123-131.
[33] Su XL, Zhan X, Tu J, "GNSS Constellation Integrity Evaluation Based on Quality Control," *Journal of Aeronautics, Astronautics and Aviation*, Vol. 48, 2016, pp. 37-46.
[34] Ding Y, Yang J, Hao Y, "A Review on Coordinated Control of Formation Configuration of Space Solar Power Station Energy Transmission System," *Journal of Aeronautics, Astronautics and Aviation*, Vol. 54, 2022, pp. 49-65.
[35] Weng SL, Lian YY, "Dynamical Modelling of FORMOSAT-7 NB-Satellite Multibody System," *Journal of Aeronautics, Astronautics and Aviation*, Vol. 47, 2015, pp. 325-332.
[36] Lin SF, Tsai JR, Lin CL, "A Plan and Its Current Status for Taiwanese Moon Exploration: A Lunar Orbiter," *Journal of Aeronautics, Astronautics and Aviation*, Vol. 52, 2020, pp. 217-228.
[37] Huang J, Zhan X, Yang R, Lin K, "TianQin constellation formation fly initial orbital maintenance with GNSS space service volume navigation," *Journal of Aeronautics, Astronautics and Aviation*, Vol. 52, 2020, pp. 205-216.
[38] Rivkin AS, Cheng AF, "Planetary defense with the Double Asteroid Redirection Test (DART) mission and prospects," *Nature communications*, 14 (2023) 1003.
[39] Rawlin VK, Pawlik EV, "A Mercury plasma-bridge neutralizer," *Journal of Spacecraft and Rockets*, Vol. 5, 1968, pp. 814-820.
[40] Conversano RW, Becatti G, Goebel DM, Chaplin VH, "Demonstration of 13,011-h of operation of a proto-flight compact heaterless lanthanum hexaboride hollow cathode," *Acta Astronautica*, Vol. 197, 2022, pp. 53-59.
[41] Zhiwei H, Pingyang W, Zhongxi N, Zhanwen Y, Zongqi X, "Early experimental investigation of the C12A7 hollow cathode fed on iodine," *Plasma Science and Technology*, 24 (2022) 074004.
[42] Potrivitu GC, Xu L, Xu S, "A low-current LaB6 open-end knife-edge emitter hollow cathode for low-power Hall thrusters," *Plasma Sources Science and Technology*, 30 (2021) 085012.
[43] Drobny C, Wulfkühler JP, Tajmar M, "Development of a C12A7 electride hollow cathode and joint operation with a plasma thruster," 36th International Electric Propulsion Conference, 2019.
[44] Payman AR, Goebel DM, "Development of a 50-A heaterless hollow cathode for electric thrusters," *Review of Scientific Instruments*, 93 (2022) 113543.
[45] Goebel DM, Payman AR, "Heaterless 300 A lanthanum hexaboride hollow cathode," *Review of Scientific Instruments*, 94 (2023) 033506.
[46] Lev DR, Mikellides IG, Pedrini D, Goebel DM, Jorns BA, McDonald MS, "Recent progress in research and development of hollow cathodes for electric propulsion," *Reviews of Modern Plasma Physics*, Vol. 3, 2019, pp. 1-89.
[47] Goebel DM, Becatti G, Mikellides IG, Lopez Ortega A, "Plasma hollow cathodes," *Journal of Applied Physics*, 130 (2021) 050902.
[48] Goebel DM, Katz I, "Fundamentals of electric propulsion: ion and Hall thrusters," John Wiley & Sons, 2008.
[49] Dushman S, "Electron emission from metals as a function of temperature," *Physical Review*, 21 (1923) 623.
[50] Richardson OW, "The electron theory of matter," University Press, 1916.
[51] Kohl WH, Kohl WH, "Handbook of materials and techniques for vacuum devices," Springer, 1967.
[52] Schottky W, "Concerning the discharge of electrons from hot wires with delayed potential," *Annalen der Physik*, 44 (1914) 1011.
[53] Forrester AT, "Large ion beams: fundamentals of generation and propagation," 1988.
[54] Davisson C, Germer L, "The thermionic work function of tungsten," *Physical Review*, 20 (1922) 300.
[55] DuBridge LA, Roehr W, "The thermionic and photoelectric work functions of molybdenum," *Physical Review*, 42 (1932) 52.
[56] Cardwell AB, "The thermionic properties of tantalum," *Physical Review*, 47 (1935) 628.
[57] Cronin J, "Modern dispenser cathodes," IEE proceedings, 1981, pp. 19-32.
[58] Gibson JW, Haas GA, Thomas RE, "Investigation of scandate cathodes: emission, fabrication, and activation processes," *IEEE Transactions on Electron Devices*, Vol. 36, 1989, pp. 209-214.
[59] Lafferty J, "Boride cathodes," *Journal of Applied Physics*, Vol. 22, 1951, pp. 299-309.
[60] Jacobson D, Storms E, "Work function measurement of lanthanum-boron compounds," *IEEE Transactions on Plasma Science*, Vol. 6, 1978, pp. 191-199.
[61] Storms E, Mueller B, "A study of surface stoichiometry and thermionic emission using LaB6,"

Journal of Applied Physics, Vol. 50, 1979, pp. 3691-3698.

[62] Rand LP, Williams JD, "A calcium aluminate electride hollow cathode," *IEEE Transactions on Plasma Science*, Vol. 43, 2014, pp.190-194.

[63] Zou W, Khan K, Zhao X, Zhu C, Huang J, Li J, Yang Y, Song W, "Direct fabrication of C12A7 electride target and room temperature deposition of thin films with low work function," *Materials Research Express*, 4 (2017) 036408.

[64] Heiler A, Waetzig K, Tajmar M, Friedl R, Nocentini R, Fantz U, "Work function performance of a C12A7 electride surface exposed to low pressure low temperature hydrogen plasmas," *Journal of Vacuum Science & Technology A: Vacuum, Surfaces, and Films*, 39 (2021) 013002.

[65] Toda Y, Yanagi H, Ikenaga E, Kim JJ, Kobata M, Ueda S, Kamiya T, Hirano M, Kobayashi K, Hosono H, "Work Function of a Room-Temperature, Stable Electride [Ca24Al28O64] 4+(e–) 4," *Advanced Materials*, Vol. 19, 2007, pp. 3564-3569.

[66] Kirkwood DM, Gross SJ, Balk TJ, Beck MJ, Booske J, Busbaher D, Jacobs R, Kordesch ME, Mitsdarffer B, Morgan D, "Frontiers in thermionic cathode research," *IEEE Transactions on Electron Devices*, Vol. 65, 2018, pp. 2061-2071.

[67] Parakhin G, Pobbubniy R, Nesterenko A, Sinitsin A, "Low-current cathode with a bao based thermoemitter," *Procedia Engineering*, Vol. 185 2017, pp. 80-84.

[68] Barik R, Bera A, Raju R, Tanwar A, Baek., Min S, Kwon O, Sattorov M, Lee K, Park GS, "Development of alloy-film coated dispenser cathode for terahertz vacuum electron devices application," *Applied Surface Science*, Vol. 276, 2013, pp. 817-822.

[69] Vancil B, Lorr J, Schmidt V, Ohlinger W, Polk J, "Reservoir hollow cathode for electric space propulsion," *IEEE Transactions on Electron Devices*, Vol. 63, 2016, pp. 4113-4118.

[70] Goebel D, "Extending hollow cathode life for electric propulsion for long-term missions," Space 2004 Conference and Exhibit, 2004, pp. 5911.

[71] Zhao J, Gamzina D, Li N, Li J, Spear AG, Barnett L, Banducci M, Risbud S, Luhmann NC, "Scandate dispenser cathode fabrication for a high-aspect-ratio high-current-density sheet beam electron gun," *IEEE Transactions on Electron Devices*, Vol. 59, 2012, pp. 1792-1798.

[72] Cronin JL, "Practical aspects of modern dispenser cathodes," 1979.

[73] Longo R, Adler E, Falce L, "Dispenser cathode life prediction model," 1984 International Electron Devices Meeting, IEEE, 1984, pp. 318-321.

[74] Longo R, "Physics of thermionic dispenser cathode aging," *Journal of Applied Physics*, Vol. 94, 2003, pp. 6966-6975.

[75] Ageev L, Grishin S, Mikhalev V, Ogorodnikov S, Stepanov V, "Characteristics of high-current plasma sources with a hollow cathode," *Radio Engineering and Electronic Physics*, Vol. 20, 1975, pp. 1869-1873.

[76] Pelletier J, Pomot C, "Work function of sintered lanthanum hexaboride," *Applied Physics Letters*, Vol. 34, 1979, pp. 249-251.

[77] Kim V, Popov G, Arkhipov B, Murashko V, Gorshkov O, Koroteyev A, Garkusha V, Semenkin A, Tverdokhlebov S, "Electric propulsion activity in Russia," IEPC Paper, 5 (2001) 2001.

[78] Goebel DM, Crow J, Forrester A, "Lanthanum hexaboride hollow cathode for dense plasma production," *Review of Scientific Instruments*, Vol. 49, 1978, pp. 469-472.

[79] Becatti G, Goebel DM, "500-A LaB6 Hollow cathode for high power electric thrusters," *Vacuum*, 198 (2022) 110895.

[80] Joussot R, Grimaud L, Mazouffre S, "Examination of a 5 A-class cathode with a LaB6 flat disk emitter in the 2 A–20 A current range," *Vacuum*, Vol. 146, 2017, pp. 52-62.

[81] Potrivitu GC, Mazouffre S, Grimaud L, Joussot R, "Anode geometry influence on LaB6 cathode discharge characteristics," *Physics of Plasmas*, 26 (2019) 113506.

[82] Hsieh JH, Shen MM, Li YH, Huang PH, "Development of a lanthanum hexaboride hollow cathode for a magnetic octupole thruster," *Vacuum*, 214 (2023) 112146.

[83] Matsuishi S, Toda Y, Miyakawa M, Hayashi K, Kamiya T, Hirano M, Tanaka I, Hosono H, "High-Density Electron Anions in a Nanoporous Single Crystal: [Ca24Al28O64] 4+(4 e-)," *Science*, Vol. 301, 2003, pp. 626-629.

[84] Hosono H, "Exploring electro-active functionality of transparent oxide materials," *Japanese Journal of Applied Physics*, 52 (2013) 090001.

[85] Hosono H, Kim J, Toda Y, Kamiya T, Watanabe S, "Transparent amorphous oxide semiconductors for organic electronics: Application to inverted OLEDs," *Proceedings of the National Academy of Sciences*, Vol. 114, 2017, pp. 233-238.

[86] Feizi E, Ray AK, "12CaO.7Al2O3 ceramic: a review of the electronic and optoelectronic applications in display devices," *Journal of display technology*, Vol. 12, 2016, pp. 451-459.

[87] Sushko PV, Shluger AL, Hayashi K, Hirano M, Hosono H, "Electron localization and a confined electron gas in nanoporous inorganic electrides," *Physical review letters*, 91 (2003) 126401.

[88] Toda Y, Matsuishi S, Hayashi K, Ueda K, Kamiya T, Hirano M, Hosono H, "Field emission of electron anions clathrated in subnanometer-sized cages in [Ca24Al28O64] 4+(4e–)," *Advanced Materials*, Vol. 16, 2004, pp. 685-689.

[89] Kim SW, Toda Y, Hayashi K, Hirano M, Hosono H, "Synthesis of a room temperature stable 12CaO.7Al2O3 electride from the melt and its application as an electron field emitter," *Chemistry of materials*, Vol. 18, 2006, pp. 1938-1944.

[90] Toda Y, Kim SW, Hayashi K, Hirano M, Kamiya T, Hosono H, Haraguchi T, Yasuda H, "Intense thermal

field electron emission from room-temperature stable electride," *Applied Physics Letters*, 87 (2005) 254103.
[91] Gondol N, Tajmar M, "A volume-averaged plasma model for heaterless C12A7 electride hollow cathodes," *CEAS Space Journal*, (2022) 1-20.
[92] Rand L, Qian X, Williams J, "Ultra low work function, non-consumable insert for hollow cathodes formed from C12A7 electride," 57th JANNAF Propulsion Meeting, 2010.
[93] Rand LP, Waggoner RM, Williams JD, "Hollow cathode with low work function electride insert," ASME International Mechanical Engineering Congress and Exposition, 2011, pp. 317-323.
[94] Rand LP, Williams JD, "Instant start electride hollow cathode," *Structure*, 9 (2013) 11.
[95] Drobny C, Nürmberger F, Tajmar M, "Development of a compact Hall thruster with a C12A7 low-power hollow cathode," Proc. of the Space Propulsion Conference, 2016, pp. 2-6.
[96] Drobny C, Wulfkühler J, Wätzig K, Tajmar M, "Detailed work function measurements and development of a hollow cathode using the emitter material C12A7 electride," Space Propulsion Conference, Seville, Spain, 2018, pp. 14-18.
[97] Drobny C, Tajmar M, Wirz R, "Development of a C12A7 Electride Hollow Cathode," 35th International Electric Propulsion Conference, 2017, pp. 1-8.
[98] McDonald MS, Caruso NR, "Ignition and early operating characteristics of a low-current C12A7 hollow cathode," 35th International Electric Propulsion Conference (IEPC), Atlanta, GA, USA, 2017, pp. 8-12.
[99] Hua Z, Wang P, Xu Z, Yu S, "Experimental characterization of the C12A7 hollow cathode and its joint operation with a low-power Hall thruster," *Vacuum*, 192 (2021) 110443.
[100] Mikellides IG, Katz I, Goebel DM, Polk JE, "Hollow cathode theory and experiment. II. A two-dimensional theoretical model of the emitter region," *Journal of Applied Physics*, 98 (2005) 113303.
[101] Goebel D, Katz I, Watkins R, Jameson K, "Hollow cathode and keeper-region plasma measurements using ultra-fast miniature scanning probes," 40th AIAA/ASME/SAE/ASEE Joint Propulsion Conference and Exhibit, 2004, pp. 3430.
[102] Mikellides I, Katz I, Jameson K, Goebel D, "Driving processes in the orifice and near-plume regions of a hollow cathode," 42nd AIAA/ASME/SAE/ASEE Joint Propulsion Conference & Exhibit, 2006, pp. 5151.
[103] Csiky GA, "Investigation of a hollow cathode discharge plasma," AMERICAN INST. OF AERONAUTICS AND ASTRONAUTICS, ELECTRIC PROPULSION CONFERENCE, AMERICAN INST. OF AERONAUTICS AND ASTRONAUTICS, 1969.
[104] Siegfried D, Wilbur P, "An investigation of mercury hollow cathode phenomena," 13th International Electric Propulsion Conference, 1978, pp. 705.
[105] J. Matsuyama T. O., H. Takegahara, "Influence of Operating Conditions on Hollow Cathode Discharge Modes," ISTS Paper, ISTS-2004-b-17 (2004).
[106] Sakai S, Katayama T, Aoyagi J, Takegahara H, "Discharge modes and characteristics of hollow cathode," Proceedings of the 30th International Electric Propulsion Conference (IEPC), Florence, Italy, 2007, pp. 2007-2215.
[107] Georgin M, "Ionization instability of the hollow cathode plume," 2020.
[108] Goebel DM, Jameson KK, Katz I, Mikellides IG, "Plasma potential behavior and plume mode transitions in hollow cathode discharges," International Electric Propulsion Conference, IEPC Paper, 2007.
[109] Goebel DM, Jameson KK, Katz I, Mikellides IG, "Potential fluctuations and energetic ion production in hollow cathode discharges," *Physics of Plasmas*, 14 (2007) 103508.
[110] Goldman R, Gurski G, Hawersaat W, "Description of the SERT II spacecraft and mission," 8th Electric Propulsion Conference, 1970, pp. 1124.
[111] Potrivitu GC, Joussot R, Mazouffre S, "Anode position influence on discharge modes of a LaB6 cathode in diode configuration," *Vacuum*, Vol. 151, 2018, pp. 122-132.
[112] Sengupta A, Brophy J, Anderson J, Garner C, Banks B, Groh K, "An overview of the results from the 30,000 hr life test of deep space 1 flight spare ion engine," 40th AIAA/ASME/SAE/ASEE Joint Propulsion Conference and Exhibit, 2004, pp. 3608.
[113] Mikellides I, Katz I, Goebel D, Polk J, "Assessments of Hollow Cathode Wear in the Xenon Ion Propulsion System (XIPS) by Numerical Analyses and Wear Tests," 44th AIAA/ASME/SAE/ASEE Joint Propulsion Conference & Exhibit, 2008, pp. 5208.
[114] Jorns BA, Dodson C, Goebel DM, Wirz R, "Propagation of ion acoustic wave energy in the plume of a high-current LaB 6 hollow cathode," *Physical Review E*, 96 (2017) 023208.
[115] Jorns BA, Mikellides IG, Goebel DM, "Ion acoustic turbulence in a 100-A LaB 6 hollow cathode," *Physical Review E*, 90 (2014) 063106.
[116] Dodson CA, Perez-Grande D, Jorns BA, Goebel DM, Wirz RE, "Ion heating measurements on the centerline of a high-current hollow cathode plume," *Journal of Propulsion and Power*, Vol. 34, 2018, pp. 1225-1234.
[117] Ortega AL, Jorns BA, Mikellides IG, "Hollow cathode simulations with a first-principles model of ion-acoustic anomalous resistivity," *Journal of Propulsion and Power*, Vol. 34, 2018, pp. 1026-1038.
[118] Mikellides IG, Katz I, Goebel DM, Jameson KK, "Evidence of nonclassical plasma transport in hollow cathodes for electric propulsion," *Journal of Applied Physics*, 101 (2007) 063301.
[119] B.A. Jorns I. G. M., D.A. Goebel, A. Lopez Ortega, "Mitigation of energetic ions and keeper erosion in

a high-current hollow cathode," *IEPC Paper*, IEPC-2015-134 (2015).
[120] Sary G, Garrigues L, Boeuf JP, "Hollow cathode modeling: II. Physical analysis and parametric study," *Plasma Sources Science and Technology*, 26 (2017) 055008.
[121] Sary G, Garrigues L, Boeuf JP, "Hollow cathode modeling: I. A coupled plasma thermal two-dimensional model," *Plasma Sources Science and Technology*, 26 (2017) 055007.
[122] Georgin MP, Jorns BA, Gallimore AD, "Onset criterion for a turbulence-driven ionization instability in hollow cathodes," *IEPC Paper*, IEPC-2019-155 (2019).
[123] Csiky GA, "Measurements of some properties of a discharge from a hollow cathode," *National Aeronautics and Space Administration*, 1969.
[124] Nedospasov AV, "Striations," *Soviet Physics Uspekhi*, 11 (1968) 174.
[125] Pekarek L, "Ionization waves (striations) in a discharge plasma," *Soviet Physics Uspekhi*, 11 (1968) 188.
[126] Robertson HS, "Moving striations in direct current glow discharges," *Physical Review*, 105 (1957) 368.
[127] Kolobov VI, "Striations in rare gas plasmas," *Journal of Physics D: Applied Physics*, 39 (2006) R487.
[128] Georgin P, Jorns BA, Gallimore AD, "An Experimental and Theoretical Study of Hollow Cathode Plume Mode Oscillations," 2017.
[129] Jorns BA, Cusson SE, Brown Z, Dale E, "Non-classical electron transport in the cathode plume of a Hall effect thruster," *Physics of Plasmas*, 27 (2020) 022311.
[130] Becatti G, Goebel DM, Zuin M, "Observation of rotating magnetohydrodynamic modes in the plume of a high-current hollow cathode," *Journal of Applied Physics*, 129 (2021) 033304.
[131] Mikellides IG, Ortega AL, Goebel DM, Becatti G, "Dynamics of a hollow cathode discharge in the frequency range of 1–500 kHz," *Plasma Sources Science and Technology*, 29 (2020) 035003.
[132] Hara K, Sekerak MJ, Boyd ID, Gallimore AD, "Mode transition of a Hall thruster discharge plasma," *Journal of Applied Physics*, 115 (2014) 203304.
[133] Hara K, Sekerak MJ, Boyd ID, Gallimore AD, "Perturbation analysis of ionization oscillations in Hall effect thrusters," *Physics of Plasmas*, 21 (2014) 122103.
[134] Lotka AJ, "Analytical note on certain rhythmic relations in organic systems," *Proceedings of the National Academy of Sciences*, Vol. 6, 1920, pp. 410-415.
[135] Potrivitu GC, Xu S, "Evidence of the ionization instability and ion acoustic turbulence correlation in sub-ampere hollow cathodes," *Journal of Electric Propulsion*, 1 (2022) 6.
[136] Jorns BA, Hofer RR, "Plasma oscillations in a 6-kW magnetically shielded Hall thruster," *Physics of Plasmas*, 21 (2014) 053512.
[137] Tsikata S, Hara K, Mazouffre S, "Characterization of hollow cathode plasma turbulence using coherent Thomson scattering," *Journal of Applied Physics*, 130 (2021) 243304.
[138] Sengupta A, "Destructive physical analysis of hollow cathodes from the deep space 1 flight spare ion engine 30,000 hr life test," 2005.
[139] Tighe W, Freick K, Chien KR, "Performance evaluation and life test of the XIPS hollow cathode heater," 41st AIAA/ASME/SAE/ASEE Joint Propulsion Conference & Exhibit, 2005, pp. 4066.
[140] Soulas GC, "Hollow cathode heater development for the space station plasma contactor," International Electric Propulsion Conference, 1993.
[141] Rohden H, "ENDURANCE TEST OF PROEL NEUTRALIZER FOR THE RIT 10: REVIEW OF THE ACTIVITIES AT ESTEC LABORATORIES," *IEPC Paper*, (1991) 91-026.
[142] Kerslake WR, Ignaczak LR, "Development and flight history of the SERT II spacecraft," *Journal of Spacecraft and Rockets*, Vol. 30, 1993, pp. 258-290.
[143] MUELLER L, "High reliability cathode heaters for ion thrusters," 12th International Electric Propulsion Conference, 1976, pp. 1071.
[144] Wordingham CJ, Taunay PYC, Choueiri E, "Multiple-kilowatt-class graphite heater for large hollow cathode ignition," 51st AIAA/SAE/ASEE Joint Propulsion Conference, 2015, pp. 4010.
[145] McDonald M, Gallimore A, Goebel D, "Note: Improved heater design for high-temperature hollow cathodes," *Review of Scientific Instruments*, 88 (2017) 026104.
[146] Beattie J, Matossian J, "Mercury ion thruster technology," 1989.
[147] Chu E, Goebel DM, "High-current lanthanum hexaboride hollow cathode for 10-to-50-kW Hall thrusters," *IEEE Transactions on Plasma Science*, Vol. 40, 2012, pp. 2133-2144.
[148] Goebel DM, Watkins RM, Jameson KK, "LaB6 hollow cathodes for ion and Hall thrusters," *Journal of Propulsion and Power*, Vol. 23, 2007, pp. 552-558.
[149] Goebel DM, Watkins RM, "Compact lanthanum hexaboride hollow cathode," *Review of Scientific Instruments*, 81 (2010) 083504.
[150] Dan M. Goebel G. B., "High Current Hollow Cathodes for High Power Electric Thrusters," *IEPC Paper*, 2022-101 (2022).
[151] Zhongxi N, Daren Y, Hong L, Guojun Y, "Effect of the Hollow Cathode Heat Power on the Performance of an Hall-Effect Thruster," *Plasma Science and Technology*, 11 (2009) 194.
[152] Levchenko I, Bazaka K, Ding Y, Raitses Y, Mazouffre S, Henning T, Klar PJ, Shinohara S, Schein J, Garrigues L, "Space micropropulsion systems for Cubesats and small satellites: From proximate targets to furthermost frontiers," *Applied Physics Reviews*, 5 (2018) 011104.
[153] Polk J, Goebel D, Guerrero P, "Thermal characteristics of lanthanum hexaboride hollow cathodes," 34th International Electric Propulsion Conference, IEPC-2015-044, Kobe, Japan, 2015.

[154] Domonkos MT, Galliniore AD, Williams GJ "Low-current hollow cathode evaluation," 35th Joint Propulsion Conference and Exhibit, 1999, pp. 2575.
[155] Domonkos MT, "Evaluation of low-current orificed hollow cathodes," University of Michigan, 1999.
[156] Drobny C, Wulfkühler J, Tajmar M, "Characterization of a Low Current Heaterless C12A7 Electride Hollow Cathode for an Electrodynamic Tether Deorbiting Device," Proceedings of the 37th International Electric Propulsion Conference (IEPC), 2022.
[157] Gondol N, Tajmar M, "Experimental investigation of electric propulsion systems using C12A7 electride hollow cathodes," *CEAS Space Journal*, Vol. 17, 2023, pp. 413-429.
[158] Bock D, Drobny C, Laufer P, Kössling M, Tajmar M, "Development and testing of electric propulsion systems at TU Dresden," 52nd AIAA/SAE/ASEE Joint Propulsion Conference, 2016, pp. 4848.
[159] Katz I, Mikellides IG, Polk JE, Goebel DM, Hornbeck SE, "Thermal model of the hollow cathode using numerically simulated plasma fluxes," *Journal of Propulsion and Power*, Vol. 23, 2007, pp. 522-527.
[160] Polk J, Goebel D, Watkins R, Jameson K, Yoneshige L, "Characterization of hollow cathode performance and thermal behavior," 42nd AIAA/ASME/SAE/ASEE Joint Propulsion Conference & Exhibit, 2006, pp. 5150.
[161] Puchkov PM, "The low-current cathode for a small power electric propulsion," 7th European Conference for Aeronautics and Space Sciences, Milan, Italy, 2017, pp. 3-6.
[162] Saevets P, Semenenko D, Albertoni R, Scremin G, "Development of a long-life low-power Hall thruster," The 35th International Electric Propulsion Conference, 2017, pp. 1-11.
[163] Potrivitu GC, Xu L, Levchenko I, Huang S, Sun Y, Rohaizat M, Lim J, Bazaka K, Xu S, "Mode transition in a low-current LaB6 hollow cathode for electric propulsion systems for small satellites," Proceedings of the 36th International Electric Propulsion Conference, Vienna, Austria, 2019, pp. 15-20.
[164] Li F, Meng T, Ning Z, Li C, Han A, Li Y, Yu D, "Improved performance of low current hollow cathode by inserted emitter core," *Vacuum*, 207 (2023) 111492.
[165] Zhiwei H, Pingyang W, Zhuang L, Zhang X, Leichao T, "An experimental study on the degradation of the C12A7 hollow cathode," *Plasma Science and Technology*, 24 (2022) 074010.
[166] BROPHY J, GARNER C, "Tests of high current hollow cathodes for ion engines," 24th Joint Propulsion Conference, 1988, pp. 2913.
[167] BROPHY J, GARNER C, "A 5000 hour xenon hollow cathode life test," 27th Joint Propulsion Conference, 1991, pp. 2122.
[168] Polk JE, Mikellides IG, Capece AM, Katz I, "Barium depletion in hollow cathode emitters," *Journal of Applied Physics*, 119 (2016) 023303.
[169] Polk JE, Mikellides IG, Katz I, Capece AM, "Tungsten and barium transport in the internal plasma of hollow cathodes," *Journal of Applied Physics*, 105 (2009) 113301.
[170] Polk J, Mikellides i, Katz I, Capece A, "Tungsten and barium transport in the internal plasma of hollow cathodes," 44th AIAA/ASME/SAE/ASEE Joint Propulsion Conference & Exhibit, 2008, pp. 5295.
[171] Patterson MJ, Domonkos MT, Carpenter C, Kovaleski SD, "Recent development activities in hollow cathode technology," *IEPC Paper*, 270 (2001) 2001.
[172] Goebel DM, Jameson KK, Watkins RM, Katz I, Mikellides IG, "Hollow cathode theory and experiment. I. Plasma characterization using fast miniature scanning probes," *Journal of Applied Physics*, 98 (2005) 113302.
[173] Goebel DM, Jameson K, Katz I, Mikellides I, "Energetic ion production and electrode erosion in hollow cathode discharges," 2005.
[174] Tsai C, Menon M, Ryan P, Schechter D, Stirling W, Haselton H, "Long-pulse ion source for neutral-beam applications," *Review of Scientific Instruments*, Vol. 53, 1982, pp. 417-423.
[175] Rawlin V, Patterson M, Chopra A, Martin S, "High current hollow cathodes for ion thrusters," *AIAA Paper*, 1987.
[176] Friedly VJ, Wilbur PJ, "High current hollow cathode phenomena," *Journal of Propulsion and Power*, Vol. 8, 1992, pp. 635-643.
[177] Polk J, Anderson J, Brophy J, Rawlin V, Patterson M, Sovey J, Hamley J, "An overview of the results from an 8200 hour wear test of the NSTAR ion thruster," 35th Joint Propulsion Conference and Exhibit, 1999, pp. 2446.
[178] Herman D, Gallimore A, "Near Discharge Cathode Assembly Plasma Potential Measurements in a 30-cm NSTAR-type Ion Engine Admist Beam Extraction," 40th AIAA/ASME/SAE/ASEE Joint Propulsion Conference and Exhibit, 2004, pp. 3958.
[179] Brophy JR, "NASA's Deep Space 1 ion engine (plenary)," *Review of Scientific Instruments*, 73 (2002) 1071-1078.
[180] Coletti M, Gabriel S, "Insert temperature measurements of a 180A hollow cathode for the HiPER project," 48th AIAA/ASME/SAE/ASEE Joint Propulsion Conference & Exhibit, 2012, pp. 4081.
[181] Kamhawi H, Van Noord J, "Development and testing of high current hollow cathodes for high power Hall thrusters," 48th AIAA/ASME/SAE/ASEE Joint Propulsion Conference & Exhibit, 2012, pp. 4080.
[182] Plasek M, Wordingham CJ, Mata SR, Luzarraga N, Choueiri EY, Polk JE, "Experimental investigation of a large-diameter cathode," 50th AIAA/ASME/SAE/ASEE Joint Propulsion Conference & Exhibit, 2014.
[183] Plasek ML, Wordingham C, Choueiri E, "Modeling and development of the RF-controlled hollow

cathode concept," 49th AIAA/ASME/SAE/ASEE Joint Propulsion Conference, 2013, pp. 4036.
[184] Plasek ML, Wordingham CJ, Choueiri EY, "Resonant mode transition in the RF-controlled hollow cathode," 33rd International Electric Propulsion Conference, 2013.
[185] Lev D, Appel L, "Heaterless Hollow Cathode Technology - A Critical Review," 2016.
[186] Lev D, Alon G, Appel L, Seeman O, Hadas Y, "Low current heaterless hollow cathode development overview," 35th International Electric Propulsion Conference, 2017.
[187] Verhey TR, Soulas GC, Mackey JA, "Heater Validation for the NEXT-C Hollow Cathodes," International Electric Propulsion Conference, 2018.
[188] Lev D, Alon G, Appel L, "Low current heaterless hollow cathode neutralizer for plasma propulsion—Development overview," *Review of Scientific Instruments*, 90 (2019) 113303.
[189] Tighe W, Chien KR, "Hollow cathode emission and ignition characterization," IEEE International Vacuum Electronics Conference, IEEE, 2008, pp. 295-296.
[190] Hsieh JH, Li YH, Shen MM, Huang PH, "LaB6 Hollow Cathode Design and Development for Magnetic Octupole Plasma Thruster," *IEPC Paper*, 2022-137 (2022).
[191] Ozturk AE, Turkoz E, Ozgen A, Celik M, "Design and thermal analysis of the insert region heater of a lanthanum hexaboride hollow cathode," 6th International Conference on Recent Advances in Space Technologies (RAST), IEEE, 2013, pp. 607-612.
[192] Vekselman V, Krasik YE, Gleizer S, Gurovich VT, Warshavsky A, Rabinovich,"Characterization of a heaterless hollow cathode," *Journal of Propulsion and Power*, Vol. 29, 2013, pp. 475-486.
[193] Koshelev N, Loyan A, "Researching of self-heated hollow cathodes start erosion characteristics," 35th Joint Propulsion Conference and Exhibit, 1999, pp. 2863.
[194] Becatti G, Conversano RW, Goebel DM, "Demonstration of 25,000 ignitions on a proto-flight compact heaterless lanthanum hexaboride hollow cathode," *Acta Astronautica*, Vol. 178, 2021, pp. 181-191.
[195] Eichhorn H, Schoenbach K, Tessnow T, "Paschen's law for a hollow cathode discharge," *Applied Physics Letters*, Vol. 63, 1993, pp. 2481-2483.
[196] Daykin-Iliopoulos A, Gabriel S, Golosnoy I, Kubota K, Funaki I, "Investigation of heaterless hollow cathode breakdown," 2015.
[197] Forman R, "Surface studies of barium and barium oxide on tungsten and its application to understanding the mechanism of operation of an impregnated tungsten cathode," *Journal of Applied Physics*, Vol. 47, 1976, pp. 5272-5279.
[198] Daykin-Iliopoulos A, Golosnoy I, Gabriel S, "Thermal profile of a lanthanum hexaboride heaterless hollow cathode," 2017.
[199] Han X, An B, Zhang H, Meng T, Liu C, Wang F, Liu X, Liu H, Ning Z, "Temperature measurement and simulation analysis of heaterless hollow cathode during start-up process," *Journal of Physics D: Applied Physics*, 55 (2022) 465204.
[200] Ham RK, "An Experimental Investigation of Heaterless Hollow Cathode Ignition," Colorado State University, 2020.
[201] Paschen F, "Ueber die zum funkenübergang in luft: wasserstoff und kohlensäure bei verschiedenen drucken erforderliche potentialdifferenz," JA Barth, 1889.
[202] Wadhwa C, "High voltage engineering," *New Age International*, 2006.
[203] Arkhipov BA, "Development and Research of Heaterless Cathode-Neutralizer for Linear Hall Thrusters (LHD) and Plasma Ion Thrusters (PIT)," *IEPC Paper*, IEPC-97-175 (1997).
[204] Fearn D, Cox AS, Moffitt D, "An investigation of the initiation of hollow cathode discharges," ROYAL AIRCRAFT ESTABLISHMENT FARNBOROUGH (UNITED KINGDOM), 1976.
[205] Koshelev N, Loyan A, Rybalov O, "Investigation of hollow cathode for low power Hall effect thruster," 30th International Electric Propulsion Conference, Florence, Italy, 2007, pp. 17-20.
[206] Schatz M, "Heaterless ignition of inert gas ion thruster hollow cathodes," International Electric Propulsion Conference, 1985, pp. 2008.
[207] Aston G, "Hollow cathode startup using a microplasma discharge," *Review of Scientific Instruments*, Vol. 52, 1981, pp. 1259-1260.
[208] Aston G, "Hollow cathode apparatus," 1984.
[209] Radmilovic-Radjenovic M, Radjenovic B, Bojarov A, Klas M, Matejcik S, "The breakdown mechanisms in electrical discharges: the role of the field emission effect in direct current discharges in micro gaps," *Acta Physica Slovaca*, 63 (2013).
[210] Ning ZX, Zhang HG, Zhu XM, Ouyang L, Liu XY, Jiang BH, Yu DR, "10000-ignition-cycle investigation of a LaB 6 hollow cathode for 3–5-kilowatt Hall thruster," *Journal of Propulsion and Power*, Vol. 35, 2019, pp. 87-93.
[211] Lev DR, Alon G, Appel L, "A 5,000-hr heaterless hollow cathode endurance test," Joint Propulsion Conference, 2018, pp. 4426.
[212] Daykin-Iliopoulos A, Golosnoy IO, Gabriel S, "Development of a high current heaterless hollow cathode," 2018.
[213] Daykin-Iliopoulos A, Golosnoy IO, Gabriel S, Bosi F, "Characterisation of a 30 A heaterless hollow cathode," 2019.
[214] Kojima K, Yokota S, Yamasaki J, Yonaha M, Kimura T, Kawamata Y, Yasui M, "Plasma diagnostics in high current hollow cathode," *Transactions of the Japan Society for Aeronautical and Space Sciences, Aerospace Technology Japan*, Vol. 17, 2019, pp. 90-95.
[215] Cobine JD, "Gaseous Conductors," Dover Publications, 1941.

[216] Goebel DM, Polk JE, "Lanthanum hexaboride hollow cathode performance and wear testing for the asteroid redirect mission Hall thruster," 52nd AIAA/SAE/ASEE Joint Propulsion Conference, 2016, pp. 4835.
[217] Goebel DM, Chu E, "High-current lanthanum hexaboride hollow cathode for high-power Hall thrusters," *Journal of Propulsion and Power*, Vol. 30, 2014, pp. 35-40.
[218] Hall SJ, Jorns BJ, Gallimore AD, Kamhawi H, Haag TW, Mackey JA, Gilland JH, Peterson PY, Baird M, "High-power performance of a 100-kW class nested Hall thruster," International Electric Propulsion Conference (IEPC), 2017.